

Anonymous Referee #1 Received and published: 9 April 2019

Comment 1

Carbonaceous aerosols are of great importance for air quality and climate. This manuscript presents long periods measurements of EC and OC in Beijing between 2013 and 2017. The results are informative under the background of China's Clean Air Act. Although the manuscript is well written generally, some conclusions are a little bit speculative, which could be improved in the revision. Specifically, Concentrations of atmospheric compositions are influenced by both meteorology and emissions. The observed decreasing trend of OC and EC could be also attributed to changes in meteorological conditions, which was not discussed.

Response: We thank the reviewer for the constructive comments and suggestions. According to the reviewer's suggestions, we have added some meteorological information in Table S1, which is referred to in line 220 of the revised manuscript, and it is now explained in lines 219-232 why the annual average OC and EC have decreased over the years. The revised part is as below:

Benefiting from the Air Pollution Prevention and Control Action Plan and increasing atmospheric self-purification capacity (ASC, shown in Table S1), a decline in annual average concentrations is on the whole recorded. In detail, the annual average concentrations of OC peaked in 2014 and then declined from 14.5 to 7.7 $\mu\text{g}/\text{m}^3$, whereas those of EC also peaked in 2014 and then declined from 4.3 to 2.6 $\mu\text{g}/\text{m}^3$ during the study period. The decline in OC and EC concentrations is closely associated with decreasing coal consumption, increasing usage of natural gases and the implementation of a strict vehicular emission standard and increasing atmospheric self-purification capacity (Tables S1- S3).

Comment 2

The strong correlation between OC and EC are not necessarily meaning they are from same source. Primary pollutants could correlate well with each other under same meteorology. Please prove these statements with more detailed analysis.

Response: Thank you for pointing this out. For better clarity, a more detailed discussion has been added in the revised manuscript.

Primary OC and EC share a variety of common sources including vehicular emissions, coal combustion, biomass burning, etc. (Bond et al., 2013). Besides, primary OC and EC can correlate well with each other under the same meteorological conditions, as these would have similar effects

on the carbonaceous aerosols in terms of atmospheric advection and convection. However, it should be noted that EC is more stable than OC (Bond et al., 2013); the correlation between OC and EC would become gradually less significant with the enhancement of secondary OC formation when the meteorology is more favorable for complex chemical conversion of volatile organic compounds (VOCs) and secondary VOCs via gas-to-particle partitioning or heterogeneous reactions. Hence, the OC/EC ratios/correlations can indicate the impact from source types and meteorological influences to some extent (Blando and Turpin, 2000).

The above modifications can be seen in lines 477-483 of the revised manuscript.

References:

- Blando, J. and Turpin, B.: Secondary organic aerosol formation in cloud and fog droplets: a literature evaluation of plausibility, *Atmos. Environ.*, 34 (10), 1623–1632, 2000.
- Bond, T. C., Doherty, S. J. Fahey, D. W., Forster, P. M., Berntsen, T., DeAngelo, B. J., Flanner, M. G., Ghan, S., Kärcher, B., Koch, D., Kinne, S., Kondo, Y., Quinn, P. K., Sarofim, M. C., Schultz, M. G., Schulz, M., Venkataraman, C., Zhang, H., Zhang, S., Bellouin, N., Guttikunda, S. K., Hopke, P. K., Jacobson, M. Z., Kaiser, J. W., Klimont, Z., Lohmann, U., Schwarz, J. P., Shindell, D., Storelvmo, T., Warren, S. G., and Zender, C. S.: Bounding the role of black carbon in the climate system: A scientific assessment, *J. Geophys. Res-Atmos.*, 118(11), 5380–5552, 2013.

Anonymous Referee #2 Received and published: 9 April 2019

General Comments

This research is to investigate the OC and EC hourly concentration variation in Beijing, China from 2013 to 2018. Based on data, authors discussed the relationship between OC and EC, and with major air pollutants and sources via inter-annual, seasonal, weekly and diurnal variations. Finally NWR and PSCF were employed to evaluate the local and regional anthropogenic sources. In general, the data of this manuscript are informative and this paper fits the scope of ACP. Please modify the manuscript based on the following comment before ACP publication.

Response: We thank the reviewer for the constructive comments and suggestions. According to the reviewer's suggestions, we have done our best to revise our manuscript.

Comments:

1. Section 3.1, page 9, Table 2 contains a lot of data, and the source of data should be acknowledged. I could not see the importance of Table 2 in the main text, and suggest that Table 2 can be shifted to supporting information.

Response: We thank the reviewer for the comment. As suggested, Table 2 has been moved to the supplementary material.

2. Page 10, line 237, it should be "Table 3", not Table 2. In Table 3, what are the meaning for TOT and TOR? Please explain both of them by note in the table. (Same with Table 4).

Response: Thanks for pointing this out. As the original Table 2 has been removed, the original Table 3 is Table 2 now. In addition, the notes for the abbreviations TOT, TOR and EA have been added as footnotes of Tables 2 and 3 in the revised manuscript.

3. Page 10, lines 254-255, what criteria did authors classify PM_{2.5} different air quality levels as excellent, good, slightly polluted, moderately polluted, heavily polluted and severely polluted? Please specify in the text.

Response: Thanks for the comment. The criteria used to classify the air quality have been added in the revised manuscript. Air quality as Excellent, good, lightly polluted (LP), moderately polluted (MP), heavily polluted (HP) and severely polluted (SP) are based on the daily average PM_{2.5} concentration, i.e., excellent ($0 < \text{PM}_{2.5} \leq 35 \mu\text{g}/\text{m}^3$), good ($35 < \text{PM}_{2.5} \leq 75 \mu\text{g}/\text{m}^3$), lightly polluted (LP, $75 < \text{PM}_{2.5} \leq 115 \mu\text{g}/\text{m}^3$), moderately polluted (MP, $115 < \text{PM}_{2.5} \leq 150 \mu\text{g}/\text{m}^3$), heavily polluted (HP, $150 < \text{PM}_{2.5} \leq 250 \mu\text{g}/\text{m}^3$) and severely polluted (SP, $\text{PM}_{2.5} > 250 \mu\text{g}/\text{m}^3$), respectively.

4. Page 10, line 254, in Fig. 2, “White Block” label is referring to PM_{2.5} in both two figures?

Response: Thanks for the comment. It is true that the “white block” refers to the PM_{2.5} concentration in the top sub-figure in Fig. 2, while it means percentage of composition in PM_{2.5} excluding OC and EC in the bottom sub-figure in Fig. 2. The legends in Fig. 2 have been revised for better clarity in the revised manuscript.

5. Section 3.2, page 11, Fig. 4 can be part of Fig. 3. Does Fig. 4 contain special information? If yes, some more discussion related to Fig. 4 should be added. Otherwise I recommended to remove this figure.

Response: As suggested, the original Fig. 4 has been removed in the revised manuscript as it presents partially repetitive information of Fig. 3.

6. Page 11, I found quite a lot of data in Fig. 3 including OC-EC during 2002-2012, SO₂, NO₂, fire spots, please specify the data sources of all these data.

Response: Thank you for pointing this out. As advised, the sources of the data, which were not included in this study, have been added in section 2 and in lines 309-310 (He et al., 2001; Zhao et al., 2013; Ji et al., 2016; Lang et al., 2017; Tao et al., 2017) in the revised manuscript.

References:

- He, K. B., Yang, F. M., Duan, F. K., Ma Y. L.: Atmospheric particulate matter and regional complex pollution, Science Press, Beijing, China. 310-327, 2011.
- Ji, D. S., Zhang, J. K., He, J., Wang, X. J., Pang, B., Liu, Z. R., Wang, L. L., and Wang, Y. S.: Characteristics of atmospheric organic and elemental carbon aerosols in urban Beijing, China, *Atmos. Environ.*, 125, 293-306, 2016.
- Lang, J. L., Zhang, Y. Y., Zhou, Y., Cheng, S. Y., Chen, D. S., Guo, X. U., Chen, S., Li, X. X., Xing, X. F., Wang, H. Y.: Trends of PM_{2.5} and chemical composition in Beijing, 2000-2015. *Aerosol Air Qual. Res.*, 17, 412-425, 2017.
- Tao, J., Zhang, L., Cao, J., and Zhang, R.: A review of current knowledge concerning PM_{2.5} chemical composition, aerosol optical properties and their relationships across China, *Atmos. Chem. Phys.*, 17, 9485-9518, <https://doi.org/10.5194/acp-17-9485-2017>, 2017.
- Zhao, P., Dong, F., and Yang, Y.: Characteristics of carbonaceous aerosol in the region of Beijing, Tianjin, and Hebei, China, *Atmos. Environ.*, 71, 389-398, 2013.

7. Page 12, lines 302-305, authors claims that biomass burning could contribution a lot to OC and EC, please be noted that fire spots in 2012 were highest, please add some discussion in this section.

Response: Thanks for this comment. More discussion has been added in line 338-349 in the revised version: “In Fig. 3, it can be seen that the annual average EC concentration and the fire spot counts exhibit a rather similar variation from 2004 to 2017, except in the year 2012, which suggests that the EC levels are somewhat correlated with the biomass burning; this might indicate that biomass burning contributed somewhat to the EC levels. The reduction in fire spot counts from 2014 to 2017, which resulted from efforts to control the agricultural field residue burning since 2013, helped to reduce the EC concentrations to some extent, but the low EC levels during 2014-2017 are likely mostly due to the implementation of the clean air act. With regard to the anomaly in the year 2012, based on the MODIS data for this year, a very non-uniform distribution of fire spots in the BTH region was observed, with a distinct decrease of fire spot counts in Beijing, but higher fire spot counts in the southern Hebei Province; this may be ascribed to the fact that the policy of Banning Straw Burning in Summer and Autumn was executed to different degrees in the whole region, with

better implementation in the Beijing area and worse action in the other parts. (http://www.beijing.gov.cn/zfxxgk/110029/qtwj22/2012-12/11/content_357114.shtml). In addition, for the years from 2002 to 2017, the highest precipitation volume in Beijing was recorded in 2012, i.e., 733.2 mm, and the rainy days mainly occurred in the intensive straw burning periods, accounting for 76.4% of all rainy days in 2012. The frequent wet scavenging might have suppressed the EC concentrations during the intensive straw burning periods, so that the annual EC level for 2012 was comparable to those recorded from 2011 onward.”

8. Section 3.3, pages 12-14, authors separately discussed monthly and seasonal variations. Actually, I found quite a lot of data explanations are similar for both monthly and seasonal variation. Is it possible for authors to combine both to simplify the discussion?

Response: Thank you for pointing this out. We have simplified the discussion in lines 360-416 in the revised manuscript and the revised text is as follows: “Fig. S1 shows the monthly mean OC and EC concentrations at our study site for the whole 5-year period. Similar variations are observed with generally higher mean OC and EC levels in the cold season (from November to March next year when the centralized urban residential heating is provided) and lower ones in the warm season (from April to October). The highest average OC and EC concentrations were $24.1 \pm 18.7 \mu\text{g}/\text{m}^3$ in December 2016 and $9.3 \pm 8.5 \mu\text{g}/\text{m}^3$ in December 2015, respectively. However, the lowest OC and EC levels were not observed in the warm months; they were $5.0 \pm 4.6 \mu\text{g}/\text{m}^3$ in January, 2018 and $1.5 \pm 1.7 \mu\text{g}/\text{m}^3$ in December, 2017, respectively; this was associated with both frequent occurrence of cold air mass and the implementation of a winter radical pollution control action plan (Chen and Chen, 2019) in Beijing from November, 2017. Overall, the increased fuel consumption for domestic heating in addition to unfavorable meteorological conditions (lower mixing layer height, temperature inversion and calm wind) in the colder months is considered to lead to higher OC and EC levels (Ji et al., 2014). In addition, the lower air temperature in the cold months led to shifting the gas-particle equilibrium of semi-volatile organic compounds (SVOCs) into the particle phase, leading to higher OC levels. In the cold months, the cold start of vehicles (5.64 million vehicles in Beijing at the end of 2017) also increased the emission of OC. In the warm season, lower OC and

EC levels were observed, which could be attributed to the following factors: no extra energy consumed for domestic heating, strong wet scavenging by frequent precipitation occurring in these months, and more unstable atmospheric conditions favorable for pollutant dispersion; in addition, during this period, the monthly mean OC and EC concentrations generally decreased from year to year. In contrast, for the cold season, the monthly mean OC and EC concentrations did not show a clear decreasing trend from year to year. In addition to the more intensive energy consumption in the cold season, the EC and OC levels could be also be enhanced strongly by regional transport and stagnant meteorology leading to ground surface accumulation in the autumn and winter (Wang et al., 2019; Yi et al., 2019), which would counteract the efficacy of the energy structure change in the Beijing-Tianjin-Hebei region of the past few years. It is worth pointing out that, on a year to year basis, the monthly average OC and EC concentrations in the cold seasons of 2017 and 2018 were generally lower than those in 2016, demonstrating to some extent the effectiveness of the execution of the radical pollution control measures for cities on the air pollution in the Beijing-Tianjin-Hebei region. The interquartile ranges of OC and EC in the warm months were narrower than in the cold months, indicating that there was more substantial variation in concentration in the latter months. The larger variation in the colder months could be caused by the cyclic accumulation and scavenging processes. In this region, due to the cyclic accumulation and scavenging process, the concentration of particulate matter increases rapidly when the air mass back trajectories change from the northwest and north to the southwest and south over successive days in Beijing; in contrast, the concentration of particulate matter declines sharply when a cold front causes the shift of back trajectories from the southwest and south to the north and northwest (Ji et al., 2012). The successive accumulation processes are closely associated with unfavorable meteorological conditions, which gives rise to higher OC and EC concentrations, while more scavenging of aerosols by cold fronts leads to lower levels.

As to the seasonality in OC and EC, similar seasonal variations are observed in the various years with generally higher mean concentrations in autumn and winter and lower levels in spring and summer (Fig. 4). Remarkably, the OC and EC concentrations in the autumn and winter of 2017 were lower than those in the previous years. This was due to the combined effect of controlling anthropogenic emissions strictly and favorable meteorological conditions. Since September 2017, a

series of the most stringent measures within the Action Plan on Prevention and Control of Air Pollution was implemented to improve the air quality; these measures included restricting industrial production by shutting down thousands of polluting plants, suspending the work of iron and steel plants in 28 major cities and limiting the use of vehicles and reducing coal consumption as a heating source in northern China. In addition, the air quality improvement in the autumn and winter of 2017 was closely tied to frequent cold fronts accompanied by strong winds, which was favorable for dispersing the pollutants. The average OC and EC concentrations in the winter were 1.69 and 1.14, 2.17 and 1.93, 1.49 and 2.14, 2.41 and 2.29 and 0.80 and 0.88 times higher than those in the summer for 2013, 2014, 2015, 2016 and 2017, respectively. The difference in the ratios for 2017 was due to the series of the most stringent measures taking effect and favorable meteorology. The Beijing municipal government in particular has made great efforts to replace coal by natural gases and electricity-powered facilities. Besides, new energy vehicles are increasingly used to replace the gasoline vehicles.”

Reference:

Chen, H. and Chen, W.: Potential impact of shifting coal to gas and electricity for building sectors in 28 major northern cities of China, *Appl. Energ.*, 236, 1049-1061, 2019.

9. Section 3.4, page 14, lines 365-367, EC concentrations increased starting from 17:00 because of evening rush hours, I am curious why morning rush hour did not result in the increase of EC?

Response: Thank you for this comment. As indicated in the manuscript, whereby ‘other times’ stands for ‘non-night times’, “At other times, both the higher PBL height and lower traffic intensity resulted in lower EC concentrations”. It has been reported that morning peaks of OC and EC levels were higher than those during the nighttime in urban areas in the US (Rattigan et al., 2010, Kang et al., 2010), where there was no strong traffic emission of OC and EC during the nighttime. However, as regulated by the Beijing Traffic management Bureau (<http://www.bjttgl.gov.cn/zhuanti/10weihao/>), HDV and HDDT are allowed to enter the urban area inside the 5th Ring Road from 0:00 to 06:00 (local Time) in Beijing. In addition to the nocturnal

PBL effect, these high emitters contribute significantly to the high levels of OC and EC from midnight to the early morning; the OC and EC originating from the morning rush hour is not sufficiently dominant to form peaks during the 6:00-8:00 period.

References:

Kang, C. M., Koutrakis P., and Suh, H. H.: Hourly measurements of fine particulate sulfate and carbon aerosols at the Harvard-U.S. Environmental Protection Agency Supersite in Boston, *J. Air Waste Manage.*, 60:11, 1327-1334, 2010.

Rattigan, O. V., Felton, H. D., Bae, M. S., Schwab, J. J., and Demerjian, K. L.: Multi-year hourly PM_{2.5} carbon measurements in New York: Diurnal, day of week and seasonal patterns, *Atmos. Environ.*, 44(16), 2043-2053, 2010.

10. Section 3.5, similar to the above comment No. 6, please specify the data source of gaseous pollutants.

Response: Thank you for pointing this out. We have added the following text for the data sources of the gaseous pollutants in section 2.2 in the revised manuscript: “The analyzers/monitors for O₃, CO, SO₂, NO_x and PM_{2.5}, and their precision, detection limits and calibration methods have been described in detail elsewhere (Ji et al., 2014). Briefly, O₃ was measured using an ultraviolet photometric analyzer (model 49i, Thermo Fisher Scientific (Thermo), USA), CO with a gas filter correlation nondispersive infrared method analyzer (model 48i, Thermo, USA), SO₂ using a pulsed-fluorescence analyzer (model 43i, Thermo, USA), NO-NO₂-NO_x with a chemiluminescence analyzer (model 42, Thermo, USA) and PM_{2.5} using a US Environmental Protection Agency Federal Equivalent Method analyzer of PM_{2.5} (SHARP 5030, Thermo, USA).”

11. Page 18, 2nd paragraph, authors discussed the relationship between ozone and OC. It is interesting to find that O₃ at 50ug/m³ represented the highest OC, and OC increased with ozone for O₃ concentration above 100ug/m³. More discussion of the potential reasons will definitely enhance the quality of manuscript.

Response: Thank you for pointing this out. We have added the following relevant discussion and explanation on the relationship between ozone and OC in lines 541-567 in the revised manuscript: “Emissions of primary air pollutants lead through multiple pathways to the formation of ozone and secondary organic carbon (SOC) (Seinfeld and Pandis, 1998), both of which are the principal components of photochemical smog. The relationship between OC and O₃ is of use for understanding their variation and formation. The OC concentrations were highest for an O₃ concentration of 50 µg/m³, which is approximately the average O₃ concentration in Beijing in winter (Cheng et al., 2018). During the period of an O₃ concentration of 50 µg/m³, low atmospheric temperature (9.4±9.9 °C), relatively high RH (59.2±23.7 %), lower WS (1.1±0.8 m/s) and higher NO_x concentrations (72.7±57.5 ppb) were observed and a lower mixed layer height was recorded in winter (Tang et al., 2016), which were favorable for accumulation and formation of OC. A relatively lower temperature is beneficial for condensation/absorption of SVOCs into existing particles (Ji et al., 2019), which would then experience further chemical reactions to generate secondary organic aerosol (SOA). Note that a low temperature does not significantly reduce SOA formation rates (Huang et al., 2014) in the winter. In addition, processes including aqueous-phase oxidation and NO₃-radical-initiated nocturnal chemistry may contribute to or even dominate SOA formation during winter (Hallquist et al., 2009; Rollins et al., 2012; Huang et al., 2014). Hence, the above factors gave rise to the higher OC concentration at an O₃ concentration of 50 µg/m³ particularly in winter. In addition, scattering and absorbing effects of aerosols that were trapped in the lower mixed layer height led to less solar radiation reaching the ground and further restrained the O₃ formation in the cold season (Xing et al., 2017; Wang et al., 2016b). OC declined when O₃ concentrations increased from 50 to 100 µg/m³. Usually moderate O₃ concentrations accompanying lower OC concentrations are caused by increasing *T* (19.5±8.3 °C), increasing WS (2.0±1.3 m/s) and less titration of relatively lower observed NO concentrations (6.4±14.6 ppb). It can also be seen that there was a concurrent increasing trend of OC and ozone when the O₃ concentration was above 100 µg/m³, which generally occurred in the warmer season. Besides the impact of meteorological conditions, such a trend might not be dominated by gas-to-particle partitioning of low-volatility

organic compounds but by the oxidation of VOCs driven by hydroxyl radicals to generate both SOC and O₃ with relatively long lifetimes (>12 h; Wood et al., 2010)”

References:

- Hallquist, M., Wenger, J., Baltensperger, U., Rudich, Y., Simpson, D., Claeys, M., Dommen, J., Donahue, N. M., George, C., Goldstein, A. H., Hamilton, J. F., Herrmann, H., Hoffmann, T., Iinuma, Y., Jang, M., Jenkin, M. E., Jimenez, J. L., Kiendler-Scharr, A., Maenhaut, W., McFiggans, G., Mentel, Th. F., Monod, A., Prevot, A. S. H., Seinfeld, J. H., Surratt, J. D., Szmigielski, R., and Wildt, J.: The formation, properties and impact of secondary organic aerosol: current and emerging issues, *Atmospheric Chemistry and Physics* 9(14), 5155-5236, 2009.
- Huang, R. J., Zhang, Y. L., Bozzetti, C., Ho, K. F., Cao, J. J., Han, Y. M., Dällenbach, K. R., Slowik, J. G., Platt, S. M., Canonaco, F., Zotter, P., Wolf, R., Pieber, S. M., Bruns, E. A., Crippa, M., Ciarelli, G., Piazzalunga, A., Schwikowski, M., Abbaszade, G., Schnelle-Kreis, J., Zimmermann, R., An, Z. S., Szidat, S., Baltensperger, U., El Haddad, I., and Prévôt, A. S. H.: High secondary aerosol contribution to particulate pollution during haze events in China, *Nature*, 514, 218-222, 2014.
- Rollins, A. W., Browne, E. C., Min, K. E., Pusede, S. E., Wooldridge, P. J., Gentner, D. R., Goldstein, A. H., Liu, S., Day, D. A., Russell, L. M., and Cohen, R. C.: Evidence for NO_x control over nighttime SOA formation, *Science* 337(6099), 1210-1212, 2012.
- Tang, G., Zhang, J., Zhu, X., Song, T., Münkler, C., Hu, B., Schäfer, K., Liu, Z., Zhang, J., Wang, L., Xin, J., Suppan, P., and Wang, Y.: Mixing layer height and its implications for air pollution over Beijing, China, *Atmos. Chem. Phys.*, 16, 2459-2475, 2016.
- Wood, E. C., Canagaratna, M. R., Herndon, S. C., Onasch, T. B., Kolb, C. E., Worsnop, D. R., Kroll, J. H., Knighton, W. B., Seila, R., Zavala, M., Molina, L. T., DeCarlo, P. F., Jimenez, J. L., Weinheimer, A. J., Knapp, D. J., Jobson, B. T., Stutz, J., Kuster, W. C., Williams, E. J.: Investigation of the correlation between odd oxygen and secondary organic aerosol in Mexico City and Houston. *Atmos. Chem. Phys.* 18(10), 8947-8968, 2010.

12. Section 3.6, page 19, line 493, no Fig. 14 and 15 are in the whole manuscript.

Response: Our apologies for this error. It has been corrected and all the joint probability data are presented in the right panels of Figs. 7 and 8 in the revised manuscript.

General comments

The manuscript describe how EC and OC concentrations changed at Beijing between 2013 and 2017. Hourly EC/OC data is important and informative. However, interpretation of data is not equally robust. In some parts, discussions are very speculative. This is the main weakness of this paper. Seasonal, diurnal and interannual variations are nicely discussed. Particularly discussion of long-term variations in EC and OC concentrations, using their own data is very informative, but the part where discussion of long-term variations are extended to 2002 using literature information is not that convincing. Authors applied nonparametric wind regression to locate local sources. This is a new tool and nicely applied in this work. They also applied PSCF to identify distant sources. I do not really think distant sources can be differentiated from local ones with PSCF, because every single trajectory ends up in Beijing, which is a huge source itself.

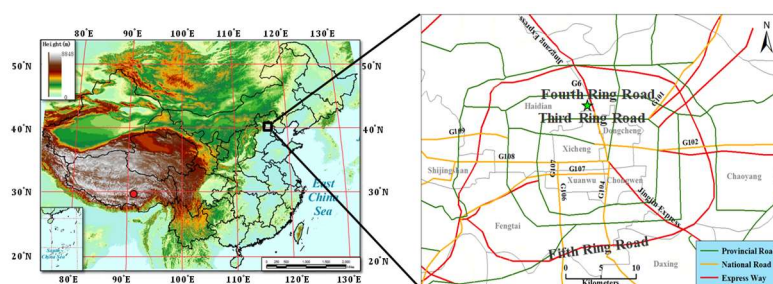
Response: We thank the reviewer for the constructive comments and suggestions. We have done our best to address all the comments and to improve our manuscript.

Specific comments

Comment 1

Figure 1. What is the "star" in the figure? Figure 1. Where is the first ring road? 4. Ring road? G6 highway? Please put these names on the map, so that reader can understand which roads you are referring to, or describe roads with notations on the map, such as, G108 etc.

Response: Thank you for pointing this out. The “star” denotes the study site. We have added the notations for the Third Ring Road, the Fourth Ring Road, the Fifth Ring Road, G6, G101, G102, G107, G108 and G109 in Fig. 1. The notations are provided near the roads and highways.



G6=Jingzang Expressway; G101=National Highway 101; G102= National Highway 102;
G107= National Highway 107; G108= National Highway 108; G109= National Highway 109

Fig.1

Comment 2

Lines 210 - 214. Authors discuss that concentrations of EC, OC and PM_{2.5} decreased from 2013 towards 2017. They should provide statistical significance of this comment. The difference between 14.0 ± 11.7 and 11.9 ± 11.3 (OC concentrations in 2013 and 2016, respectively) may or may not be statistically significant and must be tested. This comment also holds for EC and PM_{2.5} concentrations.

Response: Thank you for pointing this out. In Table 1, it can be seen that the annual average concentrations of both OC and EC peaked in 2014 and then started to decline gradually during the remainder of the study period. Nonetheless, the annual average concentration of PM_{2.5} was generally decreasing from 2013 to 2017 with a moderate peak in 2016. As advised by the reviewer, 2-tailed paired t-tests were applied for OC, EC and PM_{2.5} using their monthly average concentrations in 2013 and 2016 as paired datasets. At a confidence level of 98%, from March to October, the paired data are statistically different, indicating that the concentrations of OC, EC and PM_{2.5} declined during the above period from 2013 to 2016; however, the concentrations of OC, EC and PM_{2.5} during November and February from 2013 to 2016 are not statistically different. This part has been modified in lines 219-232 in the revised manuscript.

Comment 3

For the same discussion.

It will be better if authors should also present median concentrations of EC, OC and PM_{2.5} in table (maybe in parenthesis by the averages), which represent right-skewed data population better than average.

Response: Thank you for pointing this out. The median concentrations of EC, OC and PM_{2.5} have been added in Table 1 of the revised manuscript; as the median are lower than the averages, it can be concluded that the data populations for OC, EC and PM_{2.5} are right-skewed.

Comment 4

Line 230. "Compared to previous studies, the ratio of TC to PM_{2.5} became smaller" Last column in Table 1 suggests that TC-to-PM_{2.5} ratio did not change much between 2013 and 2018 in Beijing. Can the difference with "other" data be due to different characteristics of sampling locations, rather than time? Author's explanations with stringent measures make sense, but if that is the case shouldn't the TC/PM_{2.5} ratio decrease in five years between 2013 and 2018 at their site as well?

Response: Thank you for pointing this out. The TC/PM_{2.5} ratio is not only associated with emission sources and different environment of the sampling locations, but also depends on the formation of secondary aerosols. Following up on the reviewer's comments and suggestion, we revised the relevant discussion in lines 249-263 in the revised manuscript: "Compared to previous studies in Beijing (Table S4), the TC to PM_{2.5} ratio became smaller, indicating a relatively lower contribution from carbonaceous aerosols to PM_{2.5} in this study. The difference in the TC/PM_{2.5} ratio could be

ascribed to two factors. One factor is the difference in characteristics of sampling locations between that in our study and those in the earlier studies. However, our site and those in the previous studies used for comparison are all located in urban areas of Beijing (Chaoyang and Haidian district, respectively). It is reasonable to assume that they are affected by common sources since the surrounding environments exhibit similar features. Besides, the annual average PM_{2.5} concentrations in both districts published by the Ministry of Environmental Protection of China (<http://106.37.208.233:20035/>) were quite comparable to each other from 2013 to 2017 ($y=0.99x$, $r^2=0.92$), indicating that both areas had particle pollution of a similar degree. The second factor is that the contribution from secondary inorganic aerosols to the PM_{2.5} became more important because of a stronger atmospheric oxidation capacity (the annual average O₃ concentrations were 102, 109, 116, 119, and 136 µg/m³, respectively, from 2013 to 2017 in the Beijing-Tianjin-Hebei region; published by <http://106.37.208.233:20035/>), which could give rise to a lower TC to PM_{2.5} ratio.”

Comment 5

Line 237. Table you are referring to is Table 3 not Table 2.

Response: Our apologies for this error. We have corrected it.

Comment 6

Line 260 Authors should explanation the criteria they used to classify air quality as Excellent, good, LP, MP HP and SP

Response: Thank you for pointing this out. The criteria used to classify the air quality have been added in the revised manuscript. Air quality as Excellent, good, LP, MP, HP and SP were based on the daily average PM_{2.5} concentration, i.e., excellent ($0 < \text{PM}_{2.5} \leq 35 \mu\text{g}/\text{m}^3$), good ($35 < \text{PM}_{2.5} \leq 75 \mu\text{g}/\text{m}^3$), lightly polluted (LP, $75 < \text{PM}_{2.5} \leq 115 \mu\text{g}/\text{m}^3$), moderately polluted (MP, $115 < \text{PM}_{2.5} \leq 150 \mu\text{g}/\text{m}^3$), heavily polluted (HP, $150 < \text{PM}_{2.5} \leq 250 \mu\text{g}/\text{m}^3$) and severely polluted (SP, $\text{PM}_{2.5} > 250 \mu\text{g}/\text{m}^3$), respectively.

Comment 7

Line 271 - 305 Authors discussed long-term variation in concentrations of EC, OC, SO₂, NO₂ and tried to relate them with variations in fuel use and traffic intensity. The discussion is very speculative. Particularly, attempts to link the drop in EC concentrations in 2010 (not in OC, not in SO₂ and NO₂) to moving a steel factory to somewhere else is not convincing.

Response: Thanks for the constructive comment. For better clarity, the last paragraph of section 3.2 has been modified in lines 350-358 in the revised manuscript: “Similar to OC and EC, the annual mean SO₂ and NO₂ concentrations also showed a decreasing trend. As well-known, SO₂ originates from coal combustion and sulfur-containing oil (Seinfeld and Pandis, 1998). With the replacement of coal for industrial facilities, residential heating and cooking by clean energy (e.g., natural gases, electricity and lower sulfur content in oil), a clear decline in annual SO₂ concentrations was observed in the Beijing area starting from 2002. As compared to SO₂, the annual decreasing rate of NO₂ was relatively lower. Besides the power plants and other boilers, traffic emissions are another major source of NO₂. The rapid increase of vehicle population may partly offset the great effort in reducing coal consumption to lower the NO₂ level despite the transition to more stringent traffic emission standards.”

Comment 8

More information should be provided about data they used from literature (2002-2012). Are these data from one study and from one measurement site, or are they from combination of various studies and various sites? This is important, because what you measure also depends on location of your sampling point. For example, can the drop they observed in EC concentrations in 2010 be an artifact due to different measurement point?

Response: Thank you for pointing this out. We have added the information for the data cited from literature (2002-2012, He et al., 2001; Zhao et al., 2013; Ji et al., 2016; Lang et al., 2017; Tao et al., 2017); information about the sampling sites is given in the references. A discussion on the decline in OC and EC concentrations has been added to substantiate its validity in lines 308-328 of the revised manuscript. Considering that measurements of OC and EC were rather scarce from 2002 to 2012, the comparison of OC and EC between multiple sites cannot be used to exclude the difference caused by location of the sampling points. However, the annual average PM_{2.5} concentrations in the observation regions (Chaoyang and Haidian districts in Beijing) published by Ministry of Environmental protection, China (<http://106.37.208.233:20035/>) were very similar to each other from 2013 to 2017 ($y=0.99x$, $r^2=0.92$).

References:

- He, K. B., Yang, F. M., Duan, F. K., Ma Y. L.: Atmospheric particulate matter and regional complex pollution, Science Press, Beijing, China. 310-327, 2011.
- Ji, D. S., Zhang, J. K., He, J., Wang, X. J., Pang, B., Liu, Z. R., Wang, L. L., and Wang, Y. S.:

- Characteristics of atmospheric organic and elemental carbon aerosols in urban Beijing, China, *Atmos. Environ.*, 125, 293-306, 2016.
- Lang, J. L., Zhang, Y. Y., Zhou, Y., Cheng, S. Y., Chen, D. S., Guo, X. U., Chen, S., Li, X. X., Xing, X. F., Wang, H. Y.: Trends of PM_{2.5} and chemical composition in Beijing, 2000-2015. *Aerosol Air Qual. Res.*, 17, 412-425, 2017.
- Tao, J., Zhang, L., Cao, J., and Zhang, R.: A review of current knowledge concerning PM_{2.5} chemical composition, aerosol optical properties and their relationships across China, *Atmos. Chem. Phys.*, 17, 9485-9518, <https://doi.org/10.5194/acp-17-9485-2017>, 2017.
- Zhao, P., Dong, F., and Yang, Y.: Characteristics of carbonaceous aerosol in the region of Beijing, Tianjin, and Hebei, China, *Atmos. Environ.*, 71, 389-398, 2013.

Comment 9

Authors should also explain why only EC concentration dropped but not SO₂ when a large steel industry stopped its operations in 2010.

Response: Thank you for pointing this out. As shown in Fig. 3, from 2010 to 2011, the concentrations of OC, EC and SO₂ have decreased. It is known that the clean air act was not started yet and the emission standards for most coal-intensive industries, including thermal power plants, had not been replaced yet by more stringent standards during that period. The significant decrease in coal consumption in 2011 compared to 2010 was to be ascribed to the relocation of Shougang Corporation and a few other highly polluting industrial facilities, which could lead to a decrease in OC, EC and SO₂ levels.

Comment 10

Line 315 Does "unfavorable meteorological conditions" mean lower mixing height, slower winds? Please state. (Unfavorable met conditions are later explained in the text. It will be better if they can bring that explanation here)

Response: Thank you for pointing this out. Unfavorable meteorological conditions included a lower mixing height and lower wind speeds (Ji et al., 2014), as indicated in line 370 in the revised manuscript.

Reference:

Ji, D., Li, L., Wang, Y., Zhang, J., Cheng, M., Sun, Y., Liu, Z. R., Wang, L. L., Tang, G. Q., Hu, B., Chao, N., Wen, T. X., and Miao, H. Y.: The heaviest particulate air-pollution episodes occurred in northern China in January, 2013: Insights gained from observation, *Atmos. Environ.*, 92, 546-556, 2014.

Comment 11

Lines 318 - 326 Authors observed decreasing EC and OC concentrations in "warm" months, but no similar decreasing trend in "cold" months. This is confusing, because throughout the manuscript they mentioned about more stringent measures of coal use, switching to cleaner forms of energy production etc. These all affect EC and OC concentrations in cold season, but they observed decreasing pattern in warm season. Please explain. Please, also state in the text, how you define cold and warm seasons.

Response: Thank you for pointing this out. For better clarity, the cold season extends from November to February next year when the centralized urban residential heating is provided, and the warm season starts in April and ends in October. In the warm season, lower OC and EC levels were observed, which could be attributed to the following factors: no extra energy consumed for domestic heating, strong wet scavenging by frequent precipitation occurring in these months, and more unstable atmospheric conditions favorable for pollutant dispersion; in addition, during this period, the monthly mean OC and EC concentrations generally decreased from year to year. In contrast, in the cold season, the monthly mean OC and EC concentrations did not show a clear decreasing trend from year to year. In addition to the more intensive energy consumption in the cold season, the EC and OC levels could also be enhanced strongly by regional transport and stagnant meteorology, leading to ground surface accumulation in the autumn and winter (Wang et al., 2019; Yi et al., 2019); this would have counteracted the efficacy of the energy structure change in the Beijing-Tianjin-Hebei region in the past few years. It is worth pointing out that, on a year to year basis, the monthly average OC and EC concentrations in the cold seasons of 2017 and 2018 were generally lower than those in 2016, demonstrating to some extent the effectiveness of the execution of the radical pollution control measures for cities on the air pollution in the Beijing-Tianjin-Hebei region. The modifications can be seen in lines 360-388 of the revised manuscript.

References:

- Wang, C., An, X., Zhang, P., Sun, Z., Cui, M., and Ma, L.: Comparing the impact of strong and weak East Asian winter monsoon on PM_{2.5} concentration in Beijing, *Atmos. Res.*, 215, 165-177, 2019.
- Yi, K., Liu, J. F., Wang, X. J., Ma, J. M., Hu, J. Y., Wan, Y., Xu, J. Y., Yang H. Z., Liu, H. Z., Xiang, S. L., and Tao, S.: A combined Arctic-tropical climate pattern controlling the inter-annual climate variability of wintertime PM_{2.5} over the North China Plain. *Environ. Pollut.*, 245, 607-615, 2019.

Comment 12

Line 323. What does "cyclic accumulation and scavenging process" mean?

Response: Thank you for pointing this out. The accumulation and scavenging processes occur in cycles because of changes in air mass origin and meteorological conditions. The concentration of particulate matter increases rapidly when the air mass back trajectories change from the northwest and north to the southwest and south over successive days in Beijing; in contrast, the concentration of particulate matter declines sharply when a cold front causes a shift of back trajectories from the southwest and south to the north and northwest (Ji et al., 2012). The accumulation processes are closely associated with unfavorable meteorological conditions, which give rise to higher OC and EC concentrations, while more scavenging of aerosols by cold fronts leads to lower levels. The modifications can be seen in lines 392-398 of the revised manuscript.

Reference:

Ji, D. S., Wang, Y. S., Wang, L. L., Chen, L. F., Hu, B., Tang, G. Q., Xin, J. Y., Song, T., Wen, T. X., Sun, Y., Pan, Y. P., and Liu, Z. R.: Analysis of heavy pollution episodes in selected cities of northern China, *Atmos. Environ.*, 50, 338-348, 2012.

Comment 13

Line 371 "The amplitude of the diurnal variation in the EC concentrations was smaller in the last three years." Please support this with traffic counts.

Response: Thank you for pointing this out. It is a pity that no diurnal variations in traffic counts are available but the hourly average traffic counts in 2015, 2016 and 2017 could be found in (Beijing Transportation Annual Report, <http://www.bjtrc.org.cn/JGJS.aspx?id=5.2&Menu=GZCG>). The hourly average traffic counts in urban Beijing were 5969/hr, 5934/hr and 6049/hr in 2015, 2016 and 2017, respectively (Beijing Transportation Annual Report, <http://www.bjtrc.org.cn/JGJS.aspx?id=5.2&Menu=GZCG>). Supposedly, the small amplitude of the diurnal variation in the last three years might be related to local emission intensities; these might be significantly affected by the enforcement of a series of traffic emission control measures since 2015, including more strict restriction of emission from heavy-duty diesel vehicle public buses, wider usage of electric public buses, and scrapping of all the high-emitting (yellow-labelled) vehicles, etc. (Table S2). All these actions led to a decline in emissions of OC and EC and narrowed the amplitude of the diurnal variation in the EC concentration.

Comment 14

Line 393. "OC and EC exhibited higher concentrations on weekends than on weekdays" Statistical significance of the difference between 13.2 ± 1.8 (OC in WE) and 11.8 ± 1.8 (OC in WD) and between 3.9 ± 2.7 (EC in WE) and 3.6 ± 3.5 (EC in WD) must be tested. These numbers are close to each other.

Response: Thanks for the comment. The difference in OC and EC concentrations between weekends and weekdays was found to be statistically significant based on the analysis of the weekly data using *t*-test statistics. Hence, the above statement was modified in line 463 in the revised manuscript: OC and EC statistically ($p < 0.05$) exhibited higher concentrations on weekends than on weekdays in this study.

Comment 15

Also, please check the standard deviations, given for OC in both WD and WE. They are too small to be real.

Response: Thanks for pointing this out. The standard deviations of OC in both WD and WE have been double checked and the correct average concentrations should be 13.2 ± 11.8 and 11.8 ± 10.8 $\mu\text{g}/\text{m}^3$ for WD and WE, respectively. The related parts have been changed in lines 464 and 466 in the revised manuscript.

Comment 16

Line 434 "This could be because vehicular emissions became the dominant pollution source and gradually replaced the industrial emissions in Beijing". Hand-waving. Must be removed.

Response: Thank you for pointing this out. This sentence is indeed very speculative and has been removed as suggested.

Comment 17

Line 489 "... highlighting probable trans-boundary transport from highly industrialized regions upwind of the Hebei province of China ...", NWR is performed using surface meteorological data. How correct is it to infer long-distance transport with surface met data? Please explain in the text.

Response: Thank you for pointing this out. As the NWR analysis provides an allocation of local sources, we feel that it is inappropriate to infer the impact of long-range transport of air masses on the studied site. Hence, the trans-boundary transport inferred from the NWR results has been removed in the revised manuscript.

Comment 18

Line 493 "The joint probability data in Figs. 14 and 15 show...." There is only 10 figures in this paper.

Response: Our apologies for this error. We have modified them. All the joint probability data are shown in the right panels in Figs. 7 and 8.

Comment 19

Line 500 "Considering that the NWR analysis can only provide an allocation of local sources, the PSCF analysis is a helpful complement to investigate potential advection of pollution over larger geographical scales" How realistic is it to attempt to locate distant sources using PSCF in the middle of a huge source like Beijing? No matter where they are coming from, all trajectories will end up in Beijing and will pick up pollutants emitted in Beijing. If every single trajectory is effected emissions in Beijing, it will be very difficult (probably impossible) to differentiate information trajectories carry about distant sources. If you agree with me, please remove PSCF from manuscript. If you do not agree with me, please explain how you avoid this drawback in the text.

Response: Thanks for this comment, but we still believe that potential source contribution function (PSCF) is a useful tool to pinpoint non-nearby potential source areas, from which the air masses can affect the acceptor site via transboundary transport. It is extensively used in the literature for pinpointing non-nearby source areas; according to the Web of Science there are currently 465 publications in which "potential source contribution function" or PSCF was used. The detailed explanation of PSCF is as follows. PSCF is one type of residence time analysis of back trajectory endpoints within a fixed space, which provides the conditional probability that a given grid cell is within the source region of the pollutant species of interest if air mass trajectories passing through the cell give rise at the receptor site to measured levels of the pollutant above a pre-defined threshold value (Sofowote et al., 2011). Consequently, PSCF analysis is able to identify geographically-disperse source regions and the preferred pathways of contaminant species to a receptor site. In this study, we selected 48-h trajectories terminating at Beijing at a height of 100 m using the Trajstat software (Wang et al., 2009). 48-h trajectories with long pathways suggest that they have a rapid moving speed corresponding with relatively higher surface WS. When trajectories with long pathways are accompanied with a higher loading of the species of interest, it suggests that regional transport has an effect on the loading of species of interest at the receptor site. The PSCF calculations were performed on a longitude-latitude grid which covers the spatial domain of interest. We assume that a species emitted within a grid cell is swept into the air parcel and transported to the receptor

site without loss through diffusion, chemical transformation or atmospheric scavenging. Let n_{ij} be the total number of trajectory segment endpoints falling in the grid cell (i, j) over the period of study, and let m_{ij} be the number of endpoints in (i, j) corresponding to trajectories associated with concentration values at the receptor site exceeding a specified threshold. The ratio, multiplied with a weighing factor, is then the conditional probability $PSCF(i, j)$ that an air parcel passing over the cell (i, j) on its way to the receptor site arrives at the site with a concentration value above the threshold. Hence, high values in the spatial distribution of $PSCF(i, j)$ will pinpoint geographical regions that are likely to produce high concentration values at the receptor site. In order to identify the high $PSCF$ values that might have arisen purely by chance, it is necessary to test these values against the null hypothesis that there is no association between concentrations and trajectories. The statistical significance of the spatial distribution of the $PSCF$ values is examined by making use of a nonparametric bootstrap method. The method assumes that the concentration values are independent and identically distributed. We draw with replacement from the original concentration data set, $C = \{c_1, c_2, \dots, c_N\}$, B random subsamples of size equal to the length of the data set, $C^* = \{c_1^*, c_2^*, \dots, c_N^*\}$. We then calculate for each bootstrapped sample k the corresponding $PSCF$ spatial distribution, $W_k^*;ij$. Let $W_k^*;ij < \dots < W_{(B)}^*;ij$ be the ordered values $\{W_k^*;ij\}$ $k=1, \dots, B$, and let α be the chosen significance level. If $\{W_k^*;ij\} \geq W_{(B+1)}^*(1-\alpha/2);ij$, the null hypothesis is rejected at the $(1-\alpha)\%$ confidence level. We decided to retain for our further analysis only the $PSCF$ values satisfying the above relation. Note that if there is more than one trajectory assigned to a concentration value, the simple bootstrap on the concentration data set is equivalent to a blocked bootstrap on the trajectory set. In this study, a weighting function $w(n_{ij})$ was multiplied by the m_{ij}/n_{ij} value when n_{ij} was lower than three times of the average number of trajectory endpoints (n_{mean}) for each cell (Dimitriou and Kassomenos et al., 2015; Polissar et al., 2001). The weight function is as follows:

$$w(n_{ij}) = \begin{cases} 1.00, & 3n_{mean} < n_{ij} \\ 0.70, & 1.5n_{mean} < n_{ij} \leq 3n_{mean} \\ 0.40, & n_{mean} < n_{ij} \leq 1.5n_{mean} \\ 0.20, & n_{ij} \leq n_{mean} \end{cases}$$

The results of our $PSCF$ analysis were consistent with the emission inventory data (Zhu et al., 2018), suggesting that our $PSCF$ analysis is trustworthy.

References:

- Dimitriou, K., and Kassomenos, P., 2015. Three year study of tropospheric ozone with back trajectories at a metropolitan and a medium scale urban area in Greece. *Sci. Total Environ.* 502, 493–501.
- Petit, J. E., Favez, O., Albinet, A., and Canonaco, F.: A user-friendly tool for comprehensive evaluation of the geographical origins of atmospheric pollution: Wind and trajectory analyses. *Environ. Modell. Softw.*, 88, 183-187, 2017.
- Polissar, A.V., Hopke, P.K., Poirot, R.L.: Atmospheric aerosol over Vermont: chemical composition and sources. *Environ. Sci. Technol.* 35, 4604–4621, 2001.
- Sofowote, U. M., Hung, H., Rastogi, A. K., Westgate, J. N., Deluca, P. F., Su, Y. S., and McCarry, B. E.: Assessing the long-range transport of path to a sub-arctic site using positive matrix factorization and potential source contribution function. *Atmos. Environ.*, 45(4), 967-976, 2011.
- Zhu, C., Tian, H., Hao, Y., Gao, J., Hao, J., Wang, Y., Hua, S., Wang, K., and Liu, H.: A high-resolution emission inventory of anthropogenic trace elements in Beijing-Tianjin-Hebei (BTH) region of China, *Atmos. Environ.*, 191, 452-462, <https://doi.org/10.1016/j.atmosenv.2018.08.035>, 2018.

1 **Impact of air pollution control measures and regional transport on**
2 **carbonaceous aerosols in fine particulate matter in urban Beijing,**
3 **China: Insights gained from long-term measurement**

4 Dongsheng Ji^{1,2*}, Wenkang Gao^{1,2}, Willy Maenhaut^{3*}, Jun He⁴, Zhe Wang^{1,5}, Jiwei Li^{1,6}, Wupeng
5 Du⁷, Lili Wang^{1,2}, Yang Sun^{1,2}, Jinyuan Xin^{1,2}, Bo Hu^{1,2}, Yuesi Wang^{1,2*}

6 ¹ *State Key Laboratory of Atmospheric Boundary Layer Physics and Atmospheric Chemistry,*
7 *Institute of Atmospheric Physics, Chinese Academy of Sciences, Beijing, 100191, China*

8 ² *Atmosphere Sub-Center of Chinese Ecosystem Research Network, Institute of Atmospheric Physics,*
9 *Chinese Academy of Sciences, Beijing, 100191, China*

10 ³ *Department of Chemistry, Ghent University, Gent, 9000, Belgium*

11 ⁴ *Natural Resources and Environment Research Group, International Doctoral Innovation Centre,*
12 *Department of Chemical and Environmental Engineering, University of Nottingham Ningbo China,*
13 *Ningbo, 315100, China*

14 ⁵ *Research Institute for Applied Mechanics, Kyushu University, Fukuoka, 816-8580, Japan*

15 ⁶ *University of Chinese Academy of Sciences, Beijing, 100049, China*

16 ⁷ *Institute of Urban Meteorology, Chinese Academy of Meteorological Sciences, Beijing, 100081,*
17 *China*

18

19 Correspondence to: Dongsheng Ji (jds@mail.iap.ac.cn), Willy Maenhaut (Willy.Maenhaut@UGent.be)
20 and Yuesi Wang (wys@dq.cern.ac.cn)

21

22 **Abstract** As major chemical components of airborne fine particulate matter (PM_{2.5}), organic carbon
23 (OC) and elemental carbon (EC) have vital impacts on air quality, climate change, and human health.
24 Because OC and EC are closely associated with fuel combustion, it is helpful for the scientific
25 community and policymakers assessing the efficacy of air pollution control measures to study on
26 the impact of the control measures and regional transport on the OC and EC levels. In this study,
27 hourly mass concentrations of OC and EC associated with PM_{2.5} were semi-continuously measured
28 from March 2013 to February 2018. The results showed that annual mean OC and EC concentrations
29 declined from 14.0 to 7.7 µg/m³ and from 4.0 to 2.6 µg/m³, respectively, from March 2013 to
30 February 2018. In combination with the data of OC and EC in previous studies, an obvious
31 decreasing trend in OC and EC concentrations was found, which was caused by clean energy
32 policies and effective air pollution control measures. However, no obvious change in the ratios of
33 OC and EC to the PM_{2.5} mass (on average, 0.164 and 0.049, respectively) was recorded, suggesting
34 that inorganic ions still contributed a lot to PM_{2.5}. Based on the seasonal variations of OC and EC,
35 it appeared that higher OC and EC concentrations were still observed in the winter months, with the
36 exception of winter of 2017-2018. Traffic policies executed in Beijing resulted in nighttime peaks
37 of OC and EC, caused by heavy-duty vehicles and heavy-duty diesel vehicles being permitted to
38 operate from 0:00 to 6:00. In addition, the fact that there was no traffic restriction in weekends led
39 to higher concentrations in weekends compared to weekdays. Significant correlations between OC
40 and EC were observed throughout the study period, suggesting that OC and EC originated from
41 common emission sources, such as exhaust of vehicles and fuel combustion. OC and EC levels
42 increased with enhanced SO₂, CO and NO_x concentrations while the O₃ and OC levels enhanced
43 simultaneously when O₃ concentrations were higher than 50 µg/m³. Nonparametric wind regression
44 analysis was performed to examine the sources of OC and EC in the Beijing area. It was found that
45 there were distinct hot spots in the northeast wind sector at wind speeds of approximately 5 km/h,
46 as well as diffuse signals in the southwestern wind sectors. Source areas further away from Beijing
47 were assessed by potential source contribution function (PSCF) analysis. A high-potential source
48 area was precisely pinpointed, which was located in the northwestern and southern areas of Beijing
49 in 2017 instead of solely in the southern areas of Beijing in 2013. This work shows that improvement
50 of the air quality in Beijing benefits from strict control measures; however, joint prevention and

51 control of regional air pollution in the regions is needed for further improving the air quality. The
52 results provide a reference for controlling air pollution caused by rapid economic development in
53 developing countries.

54

55 **Key words** air pollution control measures, regional transport, organic carbon, elemental carbon,
56 Beijing

57

58 **1 Introduction**

59 Worldwide attention on atmospheric organic carbon (OC) and elemental carbon (EC) has been
60 paid by the public and the scientific community because OC and EC have vital effects on air quality,
61 atmospheric visibility, climate, and human health (Bond et al., 2013; Boucher et al., 2013; World
62 Health Organization (WHO), 2012). OC is composed of thousands of organic compounds and
63 occupies 10-50 % of the ambient PM_{2.5} mass (Seinfeld and Pandis, 1998) while EC, which is emitted
64 from fuel combustion, represents 1-13 % of the ambient PM_{2.5} mass (Shah et al., 1986; Tao et al.,
65 2017; Malm et al., 1994). Considering that OC and EC occupy high fractions of the PM_{2.5}, a decline
66 in OC and EC concentrations will improve air quality. Due to the light scattering potential of OC
67 and the light absorption ability of EC, high concentrations of OC and EC can impair the atmospheric
68 visibility. In addition, OC and EC can affect the atmospheric energy balance through scattering and
69 absorbing incoming and outgoing solar and terrestrial radiation (direct effect) and through
70 modifying the microphysical properties of clouds, like influencing cloud condensation nuclei and/or
71 ice nuclei (indirect effects). Direct and indirect effects of OC and EC remain one of the principal
72 uncertainties in estimates of anthropogenic radiative forcing (Boucher et al., 2013). In particular,
73 black carbon (BC also called EC) coated with secondary particles can enhance aerosol radiative
74 forcing (Wang et al., 2013; Zhang et al., 2008). BC is found to aggravate haze pollution in megacities
75 (Ding et al., 2016; Zhang et al., 2018). Most of all, OC and EC adversely affect human health. As
76 important constituents of OC, polycyclic aromatic hydrocarbons (PAHs) are well known as
77 carcinogens, mutagens, and teratogens and therefore pose a serious threat to the health and the well-
78 being of humans (Boström et al., 2002). Short-term epidemiological studies provide sufficient
79 evidence of all-cause and cardiovascular mortality and cardiopulmonary hospital admissions
80 associated with daily variations in BC concentrations; besides, cohort studies proved that all-cause
81 and cardiopulmonary mortality are linked with long-term average BC exposure (WHO, 2012). Thus,
82 long-term continuous observations of OC and EC are a prerequisite to further study air quality,
83 atmospheric visibility, climate effects, and human health. However, long-term continuous
84 observations of OC and EC in China are scarce.

85 In the world, China is considered as one of the regions of high emissions of OC and EC due to
86 high energy consumption and increasing vehicle population, accompanying rapid economic

87 development and urbanization for decades (<http://www.stats.gov.cn/tjsj/ndsj/2017/indexch.htm>). As
88 the capital of China, Beijing with a residential population of 21.7 million, domestic tourists of
89 2.9×10^2 million and foreign tourists of approximately 3.3 million in 2017
90 (<http://tjj.beijing.gov.cn/English/AD/>) faces severe air pollution problems, which have attracted
91 worldwide attention. A series of studies on OC and EC have already been performed in Beijing.
92 Lang et al. (2017) indicated that OC showed a downward trend and EC had almost no change before
93 2003, both increased from 2003 to 2007, but decreased after 2007. The decline in OC concentrations
94 was associated with coal combustion and motor vehicle emission control measures, while that in
95 EC was caused by the replacement of fossil fuel and control of biomass emissions. Tao et al. (2017)
96 stated that the nearly 30 % reduction in total carbon (TC) in recent years in Beijing can be taken as
97 a real trend. Lv et al. (2016) found that the concentrations of OC and EC remained unchanged from
98 2000 to 2010 in Beijing. Yang et al. (2011a) conducted a long-term study of carbonaceous aerosol
99 from 2005 to 2008 in urban Beijing and found a decline in the ratio of carbonaceous species to the
100 $PM_{2.5}$ mass in contrast to what was observed 10 years earlier, which indicated that the importance
101 of carbonaceous species in $PM_{2.5}$ had decreased. In addition, pronounced seasonal variations were
102 recorded with the highest concentrations occurring in winter and the lowest ones in summer. Overall,
103 these previous researches seem somewhat inconsistent with each other and they seldom focused on
104 studying the impact of air pollution control measures and regional transport on the carbonaceous
105 aerosol levels in detail.

106 Notably, a series of the strictest measures on emission abatement and pollution control were
107 implemented in China from September 2013 (Jin et al., 2016). Substantial manpower and material
108 resources have been put into improving the air quality in the past five years and significant measures
109 are being taken for the atmospheric environment and ecosystem (Gao et al., 2017). To evaluate the
110 effectiveness of air pollution control measures, it is necessary to conduct a long-term continuous
111 observation of OC and EC and to study their long-term variation. Most of the previous studies
112 showed average information for certain periods based on filter sampling and laboratory analysis and
113 did not reflect the dynamic evolution processes of OC and EC with hourly resolution, which can
114 provide important and detailed information for the potential health risk in the area with frequent
115 occurrence of air pollution episodes. In addition, long-term measurements in urban areas of China

116 with high population density were scarce (Yang et al., 2005, 2011a; Zhang et al., 2011; Li et al.,
117 2015; Chang et al., 2017) and the knowledge on long-term continuous hourly observations is still
118 lacking, which is yet important for recognizing the influence of source emissions on air quality.

119 Based on the-above mentioned background, it is necessary to perform a long-term continuous
120 hourly observation to explore the characteristics of OC and EC, to examine the relationship between
121 OC and EC and with major air pollutants and their sources so as to better assess the influence of
122 emission control measures on the OC and EC levels. In this study, inter-annual, seasonal, weekly
123 and diurnal variation of OC and EC were investigated. The influence of local and regional
124 anthropogenic sources was evaluated using non-parametric wind regression (NWR) and potential
125 contribution source function (PSCF) methods. This study will be helpful for improving the
126 understanding of the variation and sources of OC and EC associated with PM_{2.5} and assessing the
127 effectiveness of local and national PM control measures and it provides a valuable dataset for
128 atmospheric modelling study and assessing the health risk. It also is the first time that a continuous
129 hourly measurement for a 5-year period based on the thermal-optical method is reported for urban
130 Beijing.

131 **2 Experimental**

132 **2.1 Description of the site**

133 The study site (39°58'28" N, 116°22'16" E, 44 m above ground) was set up in the second floor
134 in the campus of the State key laboratory of atmospheric boundary physics and atmospheric
135 chemistry of the Institute of atmospheric Physics, Chinese Academy of Science (Fig. 1). The site is
136 approximately 1 km south from the 3rd Ring Road (main road), 1.2 km north from the 4th Ring
137 Road (main road), 200 m west of the G6 Highway (which runs north-south) and 50 m south of the
138 Beitucheng West Road (which runs east-west), respectively. The annual average vehicular speeds in
139 the morning and evening traffic peaks were approximately 27.8 and 24.6 km/h, respectively, in the
140 past five years. During the whole study period the level of traffic congestion is mild based on the
141 traffic performance index published by the Beijing Traffic Management Bureau
142 (<http://www.bjtrc.org.cn/>), which indicated 1.5-1.8 times more time will be taken to publicly travel
143 during traffic peaks than during smooth traffic. The study site is surrounded by residential zones, a
144 street park and a building of ancient relics without industrial sources. The experimental campaign

145 was performed from March 1, 2013 to February 28, 2018. The periods of March 1, 2013 to February
146 28, 2014, March 1, 2014 to February 28, 2015, March 1, 2015 to February 28, 2016, March 1, 2016
147 to February 28, 2017 and March 1, 2017 to February 28, 2018 are, hereinafter, called for short 2013,
148 2014, 2015, 2016 and 2017, respectively.

149 **2.2 Instrumentation**

150 Concentrations of PM_{2.5}-associated OC and EC were hourly measured with semi-continuous
151 thermal-optical transmittance method OC/EC analyzers (Model 4, Sunset Laboratory Inc. Oregon,
152 Unite states of America (USA)). The operation and maintenance are strictly executed according to
153 standard operating procedures (SOP, <https://www3.epa.gov/ttnamti1/spesunset.html>). Volatile
154 organic gases are removed by an inline parallel carbon denuder installed upstream of the analyzer.
155 A round 16-mm quartz filter is used to collect PM_{2.5} with a sampling flow rate of 8 L/m. A modified
156 NIOSH thermal protocol (RT-Quartz) is used to measure OC and EC. The sampling period is 30
157 min and the analysis process lasts for 15 min. Calibration is performed according to the SOP. An
158 internal standard CH₄ mixture (5.0 %; ultra-high purity He) is automatically injected to calibrate the
159 analyzer at the end of every analysis. In addition, off-line calibration was conducted with an external
160 amount of sucrose standard (1.06 µg) every three months. The quartz fiber filters used for sample
161 collection were replaced by new ones before the laser correction factor dropped below 0.90. After
162 replacement, a blank measurement of the quartz fiber filters is carried out. The uncertainty of the
163 TC measurement has been estimated to be approximately ±20 % (Peltier et al., 2007). The
164 analyzers/monitors for O₃, CO, SO₂, NO_x and PM_{2.5}, and their precision, detection limits and
165 calibration methods have been described in detail elsewhere (Ji et al., 2014). Briefly, O₃ was
166 measured using an ultraviolet photometric analyzer (model 49i, Thermo Fisher Scientific (Thermo),
167 USA), CO with a gas filter correlation nondispersive infrared method analyzer (model 48i, Thermo,
168 USA), SO₂ using a pulsed-fluorescence analyzer (model 43i, Thermo, USA), NO-NO₂-NO_x with a
169 chemiluminescence analyzer (model 42, Thermo, USA) and PM_{2.5} using a US Environmental
170 Protection Agency Federal Equivalent Method analyzer of PM_{2.5} (SHARP 5030, Thermo, USA).
171 Meteorological data such as wind speed (WS), wind direction (WD), relative humidity (RH) and
172 atmospheric temperature (*T*) were recorded via an automatic meteorological station (Model
173 AWS310; Vaisala, Finland). The data were processed using an Igor-based software (Wu et al., 2018)

174 and the commercial software of Origin.

175 **2.3 NWR and PSCF methods**

176 **2.3.1 NWR method**

177 NWR is a source-to-receptor source identification model, which provides a meaningful
178 allocation of local sources (Henry et al., 2009; Petit et al., 2017). Wind analysis results using NWR
179 were obtained using a new Igor-based tool, named ZeFir, which can perform a comprehensive
180 investigation of the geographical origins of the air pollutants (Petit et al., 2017). The principle of
181 NWR is to smooth the data over a fine grid so that concentrations of air pollutants of interest can be
182 estimated by any couple of wind direction (θ) and wind speed (u). The smoothing is based on a
183 weighing average where the weighing coefficients are determined using a weighting function $K(\theta,$
184 $u, \sigma, h) = K_1(\theta, \sigma) \times K_2(u, h)$ (i.e., Kernel functions). The estimated value (E) given θ and u is
185 calculated by the following equations (1)-(3):

$$186 \quad E(\theta|u) = \frac{\sum_{i=1}^N K_1\left(\frac{\theta-W_i}{\sigma}\right) \times K_2\left(\frac{u-Y_i}{h}\right) \times C_i}{\sum_{i=1}^N K_1\left(\frac{\theta-W_i}{\sigma}\right) \times K_2\left(\frac{u-Y_i}{h}\right)} \quad (1)$$

$$187 \quad K_1(x) = \frac{1}{\sqrt{2\pi}} \times e^{-0.5x^2} \quad -\infty < x < \infty \quad (2)$$

$$188 \quad K_2(x) = 0.75 \times (1-x^2) \quad -1 < x < 1 \quad (3)$$

189 where σ and h were smoothing parameters, which can be suggested by clicking on the button of
190 suggest estimate in the software of Zefir; C_i , W_i , and Y_i are the observed concentration of a pollutant
191 of interest, resultant wind speed and direction, respectively, for the i th observation in a time period
192 starting at time t_i ; N is the total number of observations.

193 After the calculation, graphs of the estimated concentration and the joint probability are
194 generated. The NWR graph of the air pollutant of interest, acquired directly via the NWR calculation,
195 represents an integrated picture of the relationship of estimated concentration of the specific
196 pollutant, wind direction and wind speed. The graph of the joint probability for the wind data,
197 equivalent to a wind rose, shows the occurrence probability distribution of the wind speed and wind
198 direction.

199 **2.3.2 PSCF method**

200 The PSCF method is based on the residence time probability analysis of air pollutants of
201 interest (Ashbaugh et al., 1985). Source locations and preferred transport pathways can be identified

202 (Poirot and Wishinski, 1986; Polissar et al., 2001; Lupu and Maenhaut, 2002). The potential
203 locations of the emission sources are determined using backward trajectories. A detailed description
204 can be found in Wang et al. (2009). In principle, the PSCF is expressed using equation (4):

$$205 \quad \text{PSCF}(i, j) = w_{ij} \times (m_{ij}/n_{ij}) \quad (4)$$

206 where w_{ij} is an empirical weight function proposed to reduce the uncertainty of n_{ij} during the study
207 period, m_{ij} is the total number of endpoints in (i, j) with concentration value at the receptor site
208 exceeding a specified threshold value (the 75th percentiles for OC and EC each year were used as
209 threshold values to calculate m_{ij}) and n_{ij} is the number of back-trajectory segment endpoints that fall
210 into the grid cell (i, j) over the period of study. The National Oceanic and Atmospheric
211 Administration Hybrid Single-Particle Lagrangian Integrated Trajectory model
212 (<https://ready.arl.noaa.gov/HYSPLIT.php>) was used for calculating the 48-h backward trajectories
213 terminating at the study site at a height of 100 m every 1 h from March 1 2013 to February 28 2018.
214 In this study, the domain for the PSCF was set in the range of (30-70 °N, 65-150 °E) with the grid
215 cell size of $0.25 \times 0.25^\circ$.

216 **3 Results and discussion**

217 **3.1 Levels of OC and EC**

218 Statistics for the OC and EC concentrations from March 1, 2013 to February 28, 2018 are
219 summarized in Table 1. Benefiting from the Air Pollution Prevention and Control Action Plan and
220 increasing atmospheric self-purification capacity (ASC, shown in Table S1), a decline in annual
221 average concentrations is on the whole recorded. In detail, the annual average concentrations of both
222 OC and EC peaked in 2014 and then started to decline gradually during the remainder of the study
223 period. Nonetheless, the annual average concentrations of $\text{PM}_{2.5}$ were generally decreasing from
224 2013 to 2017. To assess whether the decreases are statistically significant, 2-tailed paired t-tests
225 were applied for OC, EC and $\text{PM}_{2.5}$ using their monthly average concentrations in 2013 and 2016
226 as paired datasets. At a confidence level of 98%, from March to October, the paired data are
227 statistically different, indicating that the concentrations of OC, EC and $\text{PM}_{2.5}$ declined during the
228 above period from 2013 to 2016; however, the concentrations of OC, EC and $\text{PM}_{2.5}$ during
229 November and February from 2013 to 2016 are not statistically different. The decline in OC and EC
230 concentrations is closely associated with decreasing coal consumption, increasing usage of natural

231 gases and the implementation of a stricter vehicular emission standard and increasing atmospheric
232 self-purification capacity (Tables S1-S3). Knowledge of the relative contribution of OC and EC to
233 PM_{2.5} is important in formulating effective control measures for ambient PM (Wang et al., 2016a).
234 The ratios of OC and EC to PM_{2.5} varied little during the whole study period, suggesting that
235 vehicular emission might be an important contributor of OC and EC although several other pollution
236 sources also contributed to the OC and EC loadings. The ratios of OC to PM_{2.5} ranged from 15.5 to
237 17.8 % with the average of 16.4 %, while those of EC to PM_{2.5} ranged from 4.5 to 5.2 % with the
238 average of 4.9 %. OC accounted, on average, for 77.0 ± 9.3 % of the total carbon (TC, the sum of
239 OC and EC), while EC amounted for 23.0 ± 9.3 % of the TC. These results are consistent with those
240 in previous studies (Wang et al., 2016a; Tao et al., 2017, Lang et al., 2017). The contribution of TC
241 to PM_{2.5}, 21.3 ± 15.8 %, is also similar to those reported in previous studies, listed in Table S4, for
242 example, at urban sites of Hongkong, China (23.5-23.6 % in 2013), Hasselt (23 %) and Mechelen
243 (24 %) in northern Belgium, rural sites in Europe (19-20 %) and some sites in India (on average,
244 20 %, Bisht et al., 2015; Ram and Sarin, 2010; Ram and Sarin, 2012), but lower than those observed
245 historically at multiple sites in China (on average 27 %, Wang et al., 2016a), with Beijing (27.6 %,
246 from March 2005 to Feb 2006), Chongqing (28.3 %, from March 2005 to February 2006), Shanghai
247 (34.5 %, from March 1999 to May 2000) and Guangzhou (26.4 %, December 2008 to February
248 2009), in Budapest (40 %), Istanbul (30 %), and many sites in the USA, like Fresno (43.2 %), Los
249 Angeles (36.9 %) and Philadelphia (33.3 %) (Na et al., 2004). Compared to previous studies in
250 Beijing (Table S4), the TC to PM_{2.5} ratio became smaller in this study, indicating a relatively lower
251 contribution from carbonaceous aerosols to PM_{2.5} in this study. The difference in the TC/PM_{2.5} ratio
252 could be ascribed to two factors. One factor is the difference in characteristics of sampling locations
253 between that in our study and those in the earlier studies. However, our site and those in the previous
254 studies used for comparison are all located in urban areas of Beijing (Chaoyang and Haidian district,
255 respectively). It is reasonable to assume that they are affected by common sources since the
256 surrounding environments exhibit similar features. Besides, the annual average PM_{2.5}
257 concentrations in both districts published by the Ministry of Environmental Protection, China
258 (<http://106.37.208.233:20035/>) were quite comparable to each other from 2013 to 2017 ($\nu=0.99x$,
259 $r^2=0.92$), indicating that both areas had particle pollution of a similar degree. The other factor is that

260 the contribution from secondary inorganic ions to the PM_{2.5} became more important because of a
261 stronger atmospheric oxidation capacity (the annual average O₃ concentrations were 102, 109, 116,
262 119, and 136 µg/m³, respectively, from 2013 to 2017 in the Beijing-Tianjin-Hebei region; published
263 by <http://106.37.208.233:20035/>), which could give rise to a lower TC to PM_{2.5} ratio. A higher TC
264 to PM_{2.5} ratio suggests that there is a lower contribution from secondary inorganic ions to PM_{2.5},
265 while a lower ratio may indicate a larger contribution from secondary inorganic ions to PM_{2.5}. The
266 carbonaceous aerosol (the sum of multiplying the measured OC by a factor of 1.4 and EC)
267 represented on average, 27.7 ± 16.7 % of the observed PM_{2.5} concentration, making it a dominant
268 contributor to PM_{2.5}.

269 Table 3 lists recently published results for OC and EC mass concentrations in major megacities.
270 Although the observation periods were not same, a comparative analysis of OC and EC
271 concentrations between different megacities could show the status of energy consumption for
272 policymakers, drawing lessons and experience from other countries. It is obvious that the PM_{2.5}-
273 associated OC and EC levels in the megacities in the developing countries were far higher than
274 those in the developed countries. The PM_{2.5}-associated OC and EC concentrations in Beijing were
275 higher than those in Athens, Greece (2.1 and 0.54 µg/m³), Los Angeles (2.88 and 0.56 µg/m³) and
276 New York (2.88 and 0.63 µg/m³), USA, Paris, France (3.0 and 1.4 µg/m³), Seoul, South Korea (4.1
277 and 1.6 µg/m³), Tokyo, Japan (2.2 and 0.6 µg/m³) and Toronto, Canada (3.39 and 0.5 µg/m³). That
278 is because clean energy has widely been used and strict control measures are taken to improve the
279 air quality step by step in the developed countries. Of the megacities in the developing countries,
280 OC and EC concentrations in Beijing were lower than those in most other megacities, like Mumbai
281 and New Delhi, India, and Xi'an and Tianjin, China, but close to those in Shanghai and Hongkong,
282 China, and higher than those in Lhasa, China. These differences/similarities indicate that OC and
283 EC gradually declined in Beijing and that a series of measures had progressive effects. However, to
284 further improve the air quality, more synergetic air pollution abatement measures of carbonaceous
285 aerosols and volatile organic compounds (VOCs) emissions need to be performed.

286 Fig. 2 shows the mass fractions of carbonaceous aerosols in different PM_{2.5} levels classified
287 according to PM_{2.5} concentrations during the whole study period. There were 571, 561, 310, 169,
288 142 and 74 days for excellent, good, slightly polluted, moderately polluted, heavily polluted and

289 severely polluted air quality levels during the whole period. It was obvious that OC and EC
290 concentrations increased with the degradation of air quality. OC and EC concentrations were 6.3
291 and 1.7, 10.2 and 2.9, 13.7 and 4.1, 17.3 and 5.3, 24.6 and 7.9 and 35.5 and 11.3 $\mu\text{g}/\text{m}^3$ for excellent,
292 good, slightly polluted (LP), moderately polluted (MP), heavily polluted (HP) and severely polluted
293 (SP) air quality days, respectively (The criteria used to classify the air quality have been added in
294 the revised manuscript. Air quality as Excellent, good, LP, MP, HP and SP were based on the daily
295 average $\text{PM}_{2.5}$ concentration, i.e., excellent ($0 < \text{PM}_{2.5} \leq 35 \mu\text{g}/\text{m}^3$), good ($35 < \text{PM}_{2.5} \leq 75 \mu\text{g}/\text{m}^3$),
296 lightly polluted (LP, $75 < \text{PM}_{2.5} \leq 115 \mu\text{g}/\text{m}^3$), moderately polluted (MP, $115 < \text{PM}_{2.5} \leq 150 \mu\text{g}/\text{m}^3$),
297 heavily polluted (HP, $150 < \text{PM}_{2.5} \leq 250 \mu\text{g}/\text{m}^3$) and severely polluted (SP, $\text{PM}_{2.5} > 250 \mu\text{g}/\text{m}^3$),
298 respectively). However, the percentages of OC and EC accounting to $\text{PM}_{2.5}$ decreased with the
299 deterioration of air quality. OC and EC made up for 31.5 % and 8.3 %, 18.9 % and 5.4 %, 14.7 %
300 and 4.4 %, 13.4 % and 4.1 %, 12.9 % and 4.2 % and 11.4 % and 3.6 % during excellent, good,
301 slightly polluted, moderately polluted, heavily polluted and severely polluted air quality days,
302 respectively. The percentage for OC decrease from 31.4 to 11.4 % while that for EC decreased from
303 8.3 to 3.6 % with the deterioration of air quality, indicating that other $\text{PM}_{2.5}$ constituents than OC
304 and EC contributed more to the increased $\text{PM}_{2.5}$ levels. This is consistent with previous studies
305 showing that secondary inorganic ions play a more important role in the increase in $\text{PM}_{2.5}$
306 concentrations (Ji et al., 2014, 2018).

307 3.2 Inter-annual variation of OC and EC

308 To evaluate the effect of the clean air act over a prolonged period, our OC and EC data were
309 combined with the data of previous studies for Beijing (He et al., 2011; Zhao et al., 2013; Ji et al.,
310 2016; Tao et al., 2017; Lang et al., 2017). As shown in Fig. 3, a decreasing trend in OC and EC
311 concentrations is on the whole observed. Table S2 summarizes a variety of policies and actions to
312 reduce pollutant emissions in power plants, coal-fired boilers, residential heating and traffic areas
313 in Beijing since 2002. Although the gross domestic product, population, energy consumption and
314 vehicular population rapidly increased (Table S3), the general decreasing trends in OC and EC
315 concentrations could be attributed to the combined effect of the more stringent traffic emission
316 standards and traffic restriction, the energy structure evolving from intensive coal and diesel
317 consumption to replacement with natural gas and electricity, and retrofitting with SO_2 and NO_2

318 removal facilities to meet the new emission standards applicable to different coal-fired facilities, etc.
319 In particular, there is an obvious dividing line of OC and EC concentrations in 2010. After 2010, the
320 OC and EC concentrations became substantially lower than those observed previously. In addition
321 to the measures mentioned in Table S2, the relocation of Shougang Corporation, which is one of the
322 China's largest steel companies, and other highly polluting factories out of Beijing might have
323 helped to some extent; all the small coal mines in Beijing were shut down and plenty of yellow label
324 (heavy-polluting) vehicles were forced off road. Note that the OC and EC levels in 2008 and 2009
325 were also somewhat lower, which was caused by a series of radical measures to improve the air
326 quality for the Olympic Games in 2008 and a decline in industrial production because of China's
327 exports crash in 2009, respectively. It suggests that a stringent clean air act and rectifying industry
328 played important roles in the air quality improvement.

329 In this study, the fire spots were counted in the domain of (30-70° N, 65-150° E) using the
330 MODIS Fire Information for Resource Management System (Giglio, 2013). Note also that the
331 effective control of biomass burning might contribute to the decrease in OC and EC concentrations.
332 In Fig. 3, it can be seen that the annual average EC concentration and fire spot counts exhibit a
333 rather similar variation from 2004 to 2017, except in the year 2012, which suggests that the EC
334 levels are somewhat correlated with the biomass burning; this might indicate that biomass burning
335 contributed somewhat to the EC levels. The reduction in fire spot counts from 2014 to 2017, which
336 resulted from efforts to control the agricultural field residue burning since 2013, helped to reduce
337 the EC concentrations to some extent, but the low EC levels during 2014-2017 are likely mostly due
338 to the implementation of the clean air act. With regard to the anomaly in the year 2012, based on
339 the MODIS data for this year, a very non-uniform distribution of fire spots in the BTH region was
340 observed, with a distinct decrease of fire spot counts in Beijing, but higher fire spot counts in the
341 southern Hebei Province; this may be ascribed to the fact that the policy of Banning Straw Burning
342 in Summer and Autumn was executed to different degrees in the whole region, with better
343 implementation in Beijing area and worse action in the other parts.
344 (http://www.beijing.gov.cn/zfxxgk/110029/qtwj22/2012-12/11/content_357114.shtml). In addition,
345 for the years from 2002 to 2017, the highest precipitation volume in Beijing was recorded in 2012,
346 i.e., 733.2 mm, and the rainy days mainly occurred in the intensive straw burning periods,

347 accounting for 76.4% of all rainy days in 2012. The frequent wet scavenging might have suppressed
348 the EC concentrations during the intensive straw burning periods, so that the annual EC level for
349 2012 was comparable to those recorded from 2011 onward.

350 Similar to OC and EC, the annual mean SO₂ and NO₂ concentrations also showed a decreasing
351 trend. As well-known, SO₂ originates from coal combustion and sulfur-containing oil (Seinfeld and
352 Pandis, 1998). With the replacement of coal for industrial facilities, residential heating and cooking
353 by clean energy (e.g., natural gases, electricity and lower sulfur content in oil), a clear decline in
354 annual SO₂ concentrations was observed in the Beijing area starting from 2002. As compared to
355 SO₂, the annual decreasing rate of NO₂ was relatively lower. Besides the power plants and other
356 boilers, traffic emissions are another major source of NO₂. The rapid increase of vehicle population
357 may partly offset the great effort in reducing coal consumption to lower the NO₂ level despite the
358 transition to more stringent traffic emission standards.

359 3.3 Monthly and seasonal variations

360 Fig. S1 shows the monthly mean OC and EC concentrations at our study site for the whole 5-
361 year period. Similar variations are observed with generally higher mean OC and EC levels in the
362 cold season (from November to February next year when the centralized urban residential heating
363 is provided) and lower ones in the warm season (from April to October). The highest average OC
364 and EC concentrations were $24.1 \pm 18.7 \mu\text{g}/\text{m}^3$ in December 2016 and $9.3 \pm 8.5 \mu\text{g}/\text{m}^3$ in December
365 2015, respectively. However, the lowest OC and EC levels were not observed in the warm months;
366 they were $5.0 \pm 4.6 \mu\text{g}/\text{m}^3$ in January, 2018 and $1.5 \pm 1.7 \mu\text{g}/\text{m}^3$ in December, 2017, respectively;
367 this was associated with both frequent occurrence of cold air mass and the implementation of a
368 winter radical pollution control action plan (Chen and Chen, 2019) in Beijing from November, 2017.
369 Overall, the increased fuel consumption for domestic heating in addition to unfavorable
370 meteorological conditions (lower mixing layer height, temperature inversion and calm wind) in the
371 colder months is considered to lead to higher OC and EC levels (Ji et al., 2014). In addition, the
372 lower air temperature in the cold months led to shifting the gas-particle equilibrium of semi-volatile
373 organic compounds (SVOCs) into the particle phase, leading to the higher OC levels. In the cold
374 months, the cold start of vehicles (5.64 million vehicles in Beijing at the end of 2017) also increased
375 the emission of OC. In the warm season, lower OC and EC levels were observed, which could be

376 attributed to the following factors: no extra energy consumed for domestic heating, strong wet
377 scavenging by frequent precipitation occurring in these months, and more unstable atmospheric
378 conditions favorable for pollutant dispersion; in addition, during this period, the monthly mean OC
379 and EC concentrations generally decreased from year to year. In contrast, for the cold season, the
380 monthly mean OC and EC concentrations did not show a clear decreasing trend from year to year.
381 In addition to the more intensive energy consumption in the cold season, the EC and OC levels
382 could also be enhanced strongly by regional transport and stagnant meteorology leading to ground
383 surface accumulation in the autumn and winter (Wang et al., 2019; Yi et al., 2019); this would have
384 counteracted the efficacy of the energy structure change in the Beijing-Tianjin-Hebei region in the
385 past few years. It is worth pointing out that, on a year to year basis, the monthly average OC and
386 EC concentrations in the cold seasons of 2017 and 2018 were generally lower than those in 2016,
387 demonstrating to some extent the effectiveness of the execution of the radical pollution control
388 measures for cities on the air pollution in the Beijing-Tianjin-Hebei region. The interquartile ranges
389 of OC and EC in the warm months were narrower than in the cold months, indicating that there was
390 more substantial variation in concentration in the latter months. The larger variation in the colder
391 months could be caused by the cyclic accumulation and scavenging processes. In this region, due to
392 these processes, the concentration of particulate matter increases rapidly when the air mass back
393 trajectories change from the northwest and north to the southwest and south over successive days in
394 Beijing; in contrast, the concentration of particulate matter declines sharply when a cold front causes
395 a shift of back trajectories from the southwest and south to the north and northwest (Ji et al., 2012).
396 The accumulation processes are closely associated with unfavorable meteorological conditions,
397 which give rise to higher OC and EC concentrations, while more scavenging of aerosols by cold
398 fronts leads to lower levels.

399 As to the seasonality in OC and EC, similar seasonal variations are observed in the various
400 years with generally higher mean concentrations in autumn and winter and lower levels in spring
401 and summer (Fig. 4). Remarkably, the OC and EC concentrations in the autumn and winter of 2017
402 were lower than those in the previous years. This was due to the combined effect of controlling
403 anthropogenic emissions strictly and favorable meteorological conditions. Since September 2017, a
404 series of the most stringent measures within the Action Plan on Prevention and Control of Air

405 Pollution was implemented to improve the air quality; these measures included restricting industrial
406 production by shutting down thousands of polluting plants, suspending the work of iron and steel
407 plants in 28 major cities and limiting the use of vehicles and reducing coal consumption as a heating
408 source in northern China. In addition, the air quality improvement in the autumn and winter of 2017
409 was closely tied to frequent cold fronts accompanied by strong winds, which was favorable for
410 dispersing the pollutants. The average OC and EC concentrations in the winter were 1.69 and 1.14,
411 2.17 and 1.93, 1.49 and 2.14, 2.41 and 2.29 and 0.80 and 0.88 times higher than those in the summer
412 for 2013, 2014, 2015, 2016 and 2017, respectively. The difference in the ratios for 2017 was due to
413 the series of the most stringent measures taking effect and favorable meteorology. The Beijing
414 municipal government in particular has made great efforts to replace coal by natural gases and
415 electricity-powered facilities. Besides, new energy vehicles are increasingly used to replace the
416 gasoline vehicles.

417 **3.4 Diurnal variation and weekly pattern for OC and EC**

418 As can be seen in Figs. S2 and S3, a clear diurnal variation is observed for both OC and EC in
419 each year. This variation is closely tied to the combined effect of diurnal variation in emission
420 strength and evolution of the PBL. The pattern for EC with higher concentrations in the nighttime
421 (from 20:00 to 4:00) and lower levels in the daytime (from 9:00 to 16:00) is largely linked to the
422 vehicular emissions. The EC concentrations increased starting from 17:00, corresponding with the
423 evening rush hours, emission from nighttime heavy-duty diesel trucks (HDDT) and heavy-duty
424 vehicles (HDV) and the formation of a nocturnal stable PBL. As regulated by the Beijing Traffic
425 management Bureau (<http://www.bjtg.gov.cn/zhuanti/10weihao/>), HDV and HDDT are allowed to
426 enter the urban area inside the 5th Ring Road from 0:00 to 06:00 (local Time). At other times, both
427 the higher PBL height and lower traffic intensity resulted in lower EC concentrations. The amplitude
428 of the diurnal variation in the EC concentrations was smaller in the last three years. The maximum
429 peak concentration (22:00-7:00) was 1.68, 1.62, 1.43, 1.40 and 1.40 times higher than that observed
430 in the valley period (13:00-15:00) for 2013, 2014, 2015, 2016 and 2017, respectively. Similar to EC,
431 the diurnal pattern for OC was also characterized by higher concentrations in the nighttime (from
432 20:00 to 4:00) and lower levels in the daytime (from 14:00 to 16:00). However, the formation of
433 secondary organic carbon from gas-phase oxidation of VOCs with increased solar radiation during

434 midday gave rise to a small additional peak of OC. Like for EC, the amplitude of the diurnal
435 variation in the OC concentrations was smaller in the last three years. The maximum peak
436 concentration (19:00-3:00) was 1.47, 1.47, 1.30, 1.34 and 1.26 times higher than that observed in
437 the valley period (14:00-16:00) for 2013, 2014, 2015, 2016 and 2017, respectively. It was pity that
438 no diurnal variation in traffic counts can be available but the hourly average traffic counts in 2015,
439 2016 and 2017 could be found in (Beijing Transportation Annual Report,
440 <http://www.bjtrc.org.cn/JGJS.aspx?id=5.2&Menu=GZCG>). Considering that the hourly average
441 traffic counts varied little in urban Beijing and they were 5969/hr, 5934/hr and 6049/hr in 2015,
442 2016 and 2017, respectively, the small amplitude of the diurnal variation in the last three years might
443 be related to local emission intensities; these might have been significantly affected by the
444 enforcement of a series of traffic emission control measures since 2015, including more strict
445 restriction of emission from heavy-duty diesel vehicle public buses, wider usage of electric public
446 buses, and scrappage of all the high-emitting (yellow-labelled) vehicles, etc. (Tab. S2). All these
447 actions led to a decline in emissions of OC and EC and narrowed the amplitude of the diurnal
448 variation in the EC concentration.

449 Separate diurnal variations of OC and EC for each season in each year are shown in Figs S4
450 and S5. Similar patterns are observed in in the four seasons but the difference between peak and
451 valley levels is larger in the winter than in the other three seasons. The larger variation in the winter
452 is due to the additional emission from residential heating and more unfavorable meteorological
453 conditions (Ji et al., 2016).

454 The difference in diurnal pattern between weekdays and weekends was also examined, see Figs.
455 S6 and S7. Similar diurnal variations are found on weekdays and weekend days. The maximum
456 peak concentration for EC (22:00-7:00) was 1.55, 1.43, 1.55, 1.51, 1.51, 1.46 and 1.59 times higher
457 than the valley concentration (13:00-15:00) for Monday, Tuesday, Wednesday, Thursday, Friday,
458 Saturday and Sunday, respectively, while the maximum peak concentration for OC (19:00-3:00)
459 was 1.41, 1.32, 1.38, 1.43, 1.37, 1.31 and 1.43 times higher than the valley concentration (14:00-
460 16:00) for Monday, Tuesday, Wednesday, Thursday, Friday, Saturday and Sunday, respectively. In
461 contrast to previous studies (Grivas et al., 2012; Jeong et al., 2017; Chang et al., 2017), OC and EC
462 exhibited statistically significant higher concentrations on weekends than on weekdays in this study

463 (statistically significant based on the analysis of the weekly data using *t*-test statistics, $p < 0.05$). The
464 average OC and EC concentrations on Saturday and Sunday were $13.2 \pm 11.8 \mu\text{g}/\text{m}^3$ and 3.9 ± 2.7
465 $\mu\text{g}/\text{m}^3$ and $12.0 \pm 10.4 \mu\text{g}/\text{m}^3$ and $3.7 \pm 3.6 \mu\text{g}/\text{m}^3$, respectively, whereas the average OC and EC
466 levels during the weekdays were $11.8 \pm 10.8 \mu\text{g}/\text{m}^3$ and $3.6 \pm 3.5 \mu\text{g}/\text{m}^3$, respectively. This indicates
467 that there is no significant decline in anthropogenic activity in the weekends compared to weekdays.
468 In fact, enhanced anthropogenic emissions could be caused by no limit on driving vehicles based
469 on license plate on weekends. The larger OC and EC concentrations in the weekend are thus mainly
470 attributed to enhanced traffic emissions, which is consistent with higher NO_2 and CO concentrations
471 in the weekend (on average $56.6 \pm 35.9 \mu\text{g}/\text{m}^3$ for NO_2 and $1.16 \pm 1.18 \text{mg}/\text{m}^3$ for CO on weekdays
472 (number of samples = 29492); $57.8 \pm 37.0 \mu\text{g}/\text{m}^3$ for NO_2 and $1.25 \pm 1.18 \text{mg}/\text{m}^3$ for CO on
473 weekends (number of samples = 11881)).

474 3.5 Relationship between OC and EC and with gaseous pollutants

475 The relationship between particulate OC and EC is an important indicator that can give
476 information on the origin and chemical transformation of carbonaceous aerosols (Chow et al., 1996).
477 Primary OC and EC are mainly derived from vehicular emissions, coal combustion, biomass
478 burning, etc. in urban areas (Bond, et al., 2013). Primary OC and EC could correlate well with each
479 other under the same meteorology. However, the correlation would become gradually less
480 significant with the enhancement of secondary OC formation via complex chemical conversion of
481 VOCs (gas-to-particle or heterogeneous conversion). In addition, it should be noted that EC is more
482 stable than OC (Bond, et al., 2013). Hence, the relationship between OC and EC can to some extent
483 be used as a parameter reflecting the source types and contributions (Blando and Turpin, 2000). Fig.
484 5 presents the regression between the OC and EC concentrations for the $\text{PM}_{2.5}$ samples of the
485 separate years 2013 to 2017. Significant correlations (R^2 ranging from 0.87 to 0.66) were observed
486 with the slopes declining from 3.6 to 2.9 throughout the study period. The significant correlations
487 suggest that in most cases OC and EC originated from similar primary sources. The slopes are
488 consistent with the OC/EC ratios ranging from 2.0 to 4.0 for urban Beijing in previous studies (He
489 et al., 2001; Dan et al., 2004; Zhao et al., 2013; Ji et al., 2016). In addition, the average OC/EC
490 ratios observed in this study are comparable to those observed at other urban sites with vehicular
491 emission as a dominant source in China and foreign countries, but lower than those in cities where

492 coal is an important source of the energy needed (Table 3). The decline in the OC/EC ratio may be
493 caused by decline in coal consumption and restriction in biomass burning. Coal combustion,
494 biomass burning and secondary formation give rise to higher OC/EC ratios while vehicular emission
495 result in lower ones (Cao et al., 2005).

496 EC and part of the OC originate from primary anthropogenic emissions, including fossil fuel
497 combustion and biomass burning (Bond et al., 2013), and secondary OC is formed along with ozone
498 formation. Hence, long-term and concurrent measurement of OC, EC, SO₂, NO_x, CO and O₃ is
499 helpful for understanding the emission features or formation processes and for providing tests to
500 current emission inventories. The variation in the OC and EC as a function of the SO₂, NO_x, CO
501 and O₃ concentration is shown in Fig. 6. There is a clear increase in OC and EC with increasing
502 SO₂, NO_x and CO, suggesting that the latter played a role in the enhancement of the former and that
503 these various species shared common sources although they have a different lifetime. OC and EC
504 increased, on average, by approximately 8.9 µg/m³ and 5.7 µg/m³, respectively, with an increase of
505 2 mg/m³ in CO. Considering that CO has a long lifetime (Liang et al., 2004) and that its increase
506 depends on source strength and meteorology, high CO concentrations usually occur in the heating
507 season when unfavorable meteorological conditions prevail. At very high CO concentrations, the
508 increase in OC becomes slower than that in EC. This can be explained by that local emissions
509 became dominant because the unfavorable meteorological conditions corresponding with the high
510 CO concentrations resulted in a weak exchange of air on the regional scale. The OC/EC ratio
511 declined at very high CO concentrations. This could be because vehicular emissions played an
512 important role in the OC and EC loadings (Ji et al., 2019). As documented by previous studies
513 (Schauer et al., 2002, Na et al., 2004), emission of gasoline vehicles results in an OC/EC ratio
514 varying from 3 to 5 while that of diesel vehicles is below 1. The above results are consistent with
515 previous studies which showed that gasoline and diesel vehicles give rise to higher CO emissions
516 (Wu et al., 2016).

517 Given that NO_x and CO have some common emission sources (Hassler et al., 2016), the OC
518 and EC levels were also analyzed in different intervals of NO_x concentrations. Both OC and EC are
519 enhanced with increasing NO_x concentrations. Their enhancements were 5.0 µg/m³ and 2.1 µg/m³,
520 respectively, for an increase in NO_x concentration of 40 µg/m³. Although NO_x are highly reactive

521 and have a short lifetime (Seinfeld and Pandis, 1998) in contrast to CO, the OC/EC ratio also
522 declined at very high NO_x concentrations, be it to a lesser extent than was the case at very high CO
523 concentrations. As was the case for high CO concentrations, more stable meteorological conditions
524 and local emissions became prevailed when higher concentrations of NO_x were observed. In fact,
525 63.5 % of all NO_x emissions come from vehicular emissions based on the statistical data of air
526 pollutant emissions in Beijing
527 (<http://www.bjepb.gov.cn/bjhrb/xxgk/ywdt/zlkz/hjtj37/827051/index.html>).

528 Examining the variation of OC and EC for different intervals of SO₂ concentrations allows us
529 to further study the impacts of industrial production or coal combustion on the OC and EC levels.
530 Similar to the relationship between CO and the carbonaceous species, the OC and EC concentrations
531 enhanced with increasing SO₂ concentrations. Their enhancements were 2.8 µg/m³ and 0.7 µg/m³,
532 respectively, for an increase in SO₂ concentration of 10 µg/m³. An increase in the OC/EC ratio
533 occurred at large SO₂ concentrations, suggesting that coal consumption provided a substantial
534 contribution to the OC and EC levels in Beijing. Because oil with a low sulfur content has been
535 widely used in Beijing since 2008 and little coal was used in the urban areas of Beijing, the SO₂
536 mostly originated from industrial production in the surrounding areas of Beijing and from coal
537 combustion for residential heating in the suburban and rural areas of Beijing. Previous studies also
538 showed that a higher OC/EC ratio is due to coal consumption and not from vehicular emissions
539 (Cao et al., 2005). Hence, coal combustion (for industrial production) on the regional scale led to
540 the enhancement of both the OC/EC ratio and SO₂ concentrations in Beijing via long-range transport.

541 Emissions of primary air pollutants lead through multiple pathways to the formation of ozone
542 and secondary organic carbon (SOC) (Seinfeld and Pandis, 1998), both of which are the principal
543 components of photochemical smog. The relationship between OC and O₃ is of use for
544 understanding their variation and formation. The OC concentrations were highest for an O₃
545 concentration of 50 µg/m³, which is approximately the average O₃ concentration in Beijing in winter
546 (Cheng et al., 2018). During the period of an O₃ concentration of 50 µg/m³, low atmospheric
547 temperature (9.4±9.9 °C), relatively high RH (59.2±23.7 %), lower WS (1.1±0.8 m/s) and higher
548 NO_x concentrations (72.7±57.5 ppb) were observed and a lower mixed layer height was recorded in
549 winter (Tang et al., 2016), which were favorable for accumulation and formation of OC. A relatively

550 lower temperature is beneficial for condensation/absorption of SVOCs into existing particles (Ji et
551 al., 2019), which would then experience further chemical reactions to generate secondary organic
552 aerosol (SOA). Note that a low temperature does not significantly reduce SOA formation rates
553 (Huang et al., 2014) in the winter. In addition, processes including aqueous-phase oxidation and
554 NO₃-radical-initiated nocturnal chemistry may contribute to or even dominate SOA formation
555 during winter (Hallquist et al., 2009; Rollins et al., 2012; Huang et al., 2014). Hence, the above
556 factors gave rise to the higher OC concentration at an O₃ concentration of 50 µg/m³ particularly in
557 winter. In addition, scattering and absorbing effects of aerosols that were trapped in the lower mixed
558 layer height led to less solar radiation reaching the ground and further restrained the O₃ formation
559 in the cold season (Xing et al., 2017; Wang et al., 2016b). OC declined when O₃ concentrations
560 increased from 50 to 100 µg/m³. Usually moderate O₃ concentrations accompanying lower OC
561 concentrations are caused by increasing *T* (19.5±8.3 °C), increasing WS (2.0±1.3 m/s) and less
562 titration of relatively lower observed NO concentrations (6.4±14.6 ppb). It can also be seen that
563 there was a concurrent increasing trend of OC and ozone when the O₃ concentration was above 100
564 µg/m³, which generally occurred in the warmer season. Besides the impact of meteorological
565 conditions, such a trend might not be dominated by gas-to-particle partitioning of low-volatility
566 organic compounds but by the oxidation of VOCs driven by hydroxyl radicals to generate both SOC
567 and O₃ with relatively long lifetimes (>12 h; Wood et al., 2010).

568 **3.6 Impact of atmospheric transport on the OC and EC concentrations**

569 **Figs. 7 and 8** show the results of the NWR analysis applied to 1-h PM_{2.5}-associated OC and
570 EC concentrations measured from 2013 and 2017 in Beijing. Fig. S8 presents the gridded emissions
571 of OC and BC for the Beijing-Tianjin-Hebei (BTH) region and China, based on emission inventory
572 (Zheng et al., 2018). The NWR results exhibit distinct hot spots (higher concentrations) in the
573 northeast wind sector at wind speeds of approximately 0-6 km/h, which were closely associated
574 with local emissions under stagnant meteorological conditions (low wind speed), as well as diffuse
575 signals in the southwestern wind sector. The joint probability data in Figs. 7 and 8 show prevailing
576 winds were from N to E and from S to W with wind speeds of approximately 1-6 km/h and of
577 approximately 4-9 km/h, respectively. Note further that the hot spots of OC are broader than those
578 of EC in the graphs of estimated concentrations; this might be due to the fact that the VOCs (the

579 precursors of SOC) emitted from upwind areas at the relatively higher WS in contrast to EC,
580 including the SW wind sector, led to an increase in OC concentrations at the receptor site while the
581 EC concentrations slowly declined due to dilution and deposition.

582 Considering that the NWR analysis can only provide an allocation of local sources, the PSCF
583 analysis is a helpful complement to investigate potential advection of pollution over larger
584 geographical scales (Petit et al., 2017). Fig. 9 presents the PSCF results for OC and EC for the years
585 2013 to 2017. Similar to the NWR analysis, the PSCF results indicated that local emissions and
586 regional transport from southerly areas were important contributors to the OC and EC loadings
587 during the whole study period. Only slight differences in the potential source regions are observed
588 between the different years. In 2013, a clear high potential source area was recorded for both OC
589 and EC; it was located in the southern plain areas of Beijing, particularly in the adjacent areas of
590 the Hebei, Henan, Shandong, Anhui and Jiangsu provinces. This was because there were intensified
591 anthropogenic emissions from those in 2013. The high pollutant emissions were caused by rapid
592 economic growth, urbanization and increase in vehicle population, energy consumption and
593 industrial activity in the southern plain areas of Beijing (Zhu et al., 2018), which resulted in a high
594 aerosol loading in the downwind areas. This result is consistent with previous studies (Ren et al.,
595 2004; Wu et al., 2014; Ji et al., 2018). In contrast to 2013, in the years 2014 to 2017 the high potential
596 source regions for OC and EC stretched to the juncture of Inner Mongolia and the Shaanxi and
597 Shanxi provinces, and even to the juncture of Inner Mongolia and the Ningxia Hui Autonomous
598 Region and of Inner Mongolia and the Gansu province. This is consistent with coal power plants
599 being abundant in the above areas (Liu F. et al., 2015). As well known, coal power plants are also
600 important emitters of SO₂, and those emissions were seen in satellite images (Li et al., 2017; Zhang
601 et al., 2017), thus proving evidence for those sources. The potential source areas for OC and EC
602 were similar in 2013 and 2014. Overall, the potential source areas were more intense for OC than
603 for EC. The emission of OC precursors (i.e., volatile organic compounds) from the Hebei, Henan,
604 Shandong, Anhui, Jiangsu, Shanxi and Shaanxi provinces led to OC concentrations downwind via
605 chemical conversion during the atmospheric transport. The widest potential source areas for OC and
606 EC were recorded in 2016 and they expanded into the eastern areas of Xinjiang Uyghur Autonomous
607 Region. They are probably associated with the economic boom in the western areas of China. In

608 2015, the potential source areas were like in 2013 and 2014 also more intense for OC than for EC.
609 Although the winter action plan was enforced in Beijing, Tianjin and 26 surrounding cities (the so-
610 called “2+26 cities”), whereby the industrial output was curtailed, inspections of polluting factories
611 were ramped up and small-scale coal burning was banned at the end of 2017, there was still a clear
612 spatial difference in emission of air pollutants, with relatively higher PM_{2.5} concentrations in the
613 southern areas of Beijing. Hence, these areas still contributed substantially to OC and EC loading
614 in Beijing.

615 As found in earlier studies (Ji et al., 2018; Zhu et al., 2018), the southern areas of Beijing were
616 main source areas. Despite the ever-stringent air pollution control measures, which are enforced in
617 key areas of China, the economic booming in the western areas of China gave rise to substantial air
618 pollution in the adjacent areas of several provinces and the northwestern areas of China. To further
619 improve the air quality in Beijing, strict emission restrictions should be launched in the above areas
620 and joint control and prevention of air pollution should be enforced on the regional scale. It should
621 be avoided that polluted enterprises, which are closed in key regions, are moved to the western areas
622 of China or to areas where there is no supervision and control of the emission of air pollutants.

623 **4 Conclusions**

624 In this study, hourly mass concentrations of OC and EC in PM_{2.5} were semi-continuously
625 measured from March 1, 2013 to February 28, 2018 at a study site in Beijing. The inter-annual,
626 monthly, seasonal and diurnal variations in OC and EC are presented, the relationship between the
627 carbonaceous species and other pollutants was examined and the source regions were assessed using
628 both NWR and PSCF analysis. The impact of the air pollution control measures and of the regional
629 transport on carbonaceous species in the fine particulate matter was investigated. The following
630 main conclusions can be drawn:

631 (1) OC and EC occupied a high fraction of the observed PM_{2.5} concentrations, making it a dominant
632 contributor of PM_{2.5}. Their concentrations increased with the degrading air quality whereas their
633 percentage in PM_{2.5} declined, which was consistent with previous studies showing that secondary
634 inorganic ions played a relatively more important role in increasing PM_{2.5} concentrations.

635 (2) A clear decline in OC and EC levels was observed after a series of energy policies for air
636 pollution abatement and control had been implemented. To further improve air quality, more

637 synergistic air pollution abatement measures of carbonaceous aerosols and VOCs emissions are
638 needed.

639 (3) OC and EC showed marked seasonal, monthly, weekly and diurnal variations. The seasonal
640 patterns were characterized by higher concentrations in the colder months (from November to
641 February) and lower ones in the warm months (from May to October) of the various years. Because
642 of stringent measures for air pollution abatement, the difference between the winter and summer
643 levels decreased. The EC diurnal pattern was characterized by higher concentrations in the nighttime
644 (from 20:00 to 4:00) and lower ones in the daytime (from 9:00 to 16:00). The higher OC and EC
645 levels during the weekend can be attributed to the traffic regulation in Beijing. The diurnal
646 fluctuation in OC and EC was closely tied to a combined effect of change in emission sources and
647 evolution of the PBL.

648 (4) Significant correlations between OC and EC were observed throughout the study period,
649 suggesting that OC and EC originated from common sources, such as vehicle exhaust, coal
650 combustion, etc. The contribution of coal combustion and biomass burning decreased and this
651 resulted in lower OC/EC ratios. The OC and EC concentrations increased with higher SO₂, CO and
652 NO_x levels, while the O₃ and OC concentrations increased simultaneously for O₃ levels above 50
653 µg/m³.

654 (5) Local emissions and regional transport played an important role in the OC and EC concentrations.
655 Higher concentrations were observed for winds from the northeast sector at wind speeds of
656 approximately 5 km/h, but there were also diffuse signals in the southwestern wind sectors. The
657 potential source regions of OC and EC stretched to the broader areas in northwestern and western
658 regions where coal and coal power plants are abundant. Some slight differences in the potential
659 source regions were observed from 2013 to 2017, which was closely associated with the economic
660 boom in the western areas of China. In addition, the southern areas of Beijing still contributed a lot
661 to OC and EC loading in Beijing.

662 In summary, this study will be helpful for improving the understanding the sources of OC and
663 EC associated with PM_{2.5} and for assessing the effectiveness of local and national PM control
664 measures. In addition, it provides valuable datasets for modelling studies and for assessing the health
665 risk.

666 **Acknowledgements**

667 This work was supported by the National Key Research and Development Program of China
668 (2017YFC0210000), the Beijing Municipal Science and Technology Projects (D17110900150000
669 and Z171100000617002), the CAS Key Technology Talent Program, and the National research
670 program for key issues in air pollution control (DQGG0101 and DQGG0102). The authors would
671 like to thank all members of the LAPC/CERN in IAP, CAS, for maintaining the instruments used in
672 the current study. We also like to thank NOAA for providing the HYSPLIT and TrajStat model.

673 **Author contributions**

674 D.S., W.M. and Y.S. designed the research. D.S., W.M., J.H., Z.W., W. K., W.P., Y.S., J.Y., B.H. and
675 Y.S. performed the research. D.S., Z.W., and W.M. analyzed the data. D.S., J.H., and W.M. wrote
676 and edited the manuscript. All other authors commented on the manuscript.

677 **References**

- 678 Ashbaugh, L. L., Malm, W. C., and Sadeh, W. Z.: A residence time probability analysis of sulfur
679 concentrations at Grand Canyon National Park, *Atmos. Environ.*, 19, 1263-1270, 1985.
- 680 Bisht, D. S., Srivastava, A. K., Pipal, A. S., Srivastava, M. K., Pandey, A. K., Tiwari, S., and
681 Pandithurai, G.: Aerosol characteristics at a rural station in southern peninsular India during
682 CAIPEEX-IGOC: physical and chemical properties, *Environ. Sci. Pollut. Res.*, 22, 5293-5304,
683 10.1007/s11356-014-3836-1, 2015.
- 684 Blando, J. and Turpin, B.: Secondary organic aerosol formation in cloud and fog droplets: a literature
685 evaluation of plausibility, *Atmos. Environ.*, 34 (10), 1623–1632, 2000.
- 686 Bond, T. C., Doherty, S. J. Fahey, D. W., Forster, P. M., Bernsten, T., DeAngelo, B. J., Flanner, M.
687 G., Ghan, S., Kärcher, B., Koch, D., Kinne, S., Kondo, Y., Quinn, P. K., Sarofim, M. C., Schultz, M.
688 G., Schulz, M., Venkataraman, C., Zhang, H., Zhang, S., Bellouin, N., Guttikunda, S. K., Hopke, P.
689 K., Jacobson, M. Z., Kaiser, J. W., Klimont, Z., Lohmann, U., Schwarz, J. P., Shindell, D., Storelvmo,
690 T., Warren, S. G., and Zender, C. S.: Bounding the role of black carbon in the climate system: A
691 scientific assessment, *J. Geophys. Res-Atmos.*, 118(11), 5380–5552, 2013.
- 692 Boström, C. E., Gerde, P., Hanberg, A., Jernström, B., Johansson, C., Kyrklund, T., Rannug, A.,
693 Tornqvist, M., Victorin, K., and Westerholm, R.: Cancer risk assessment, indicators, and guidelines

694 for polycyclic aromatic hydrocarbons in the ambient air, *Environ. Health Perspect.*, 110, 451-488,
695 2002.

696 Boucher, O., Randall, D., Artaxo, P., Bretherton, C., Feingold, G., Forster, P., Kerminen, V. M.,
697 Kondo, Y., Liao, H., Lohmann, U., Rasch, P., Satheesh, S. K., Sherwood, S., Stevens, B., Zhang, X.
698 Y.: Contribution of working group | to the fifth assessment report of the Intergovernmental Panel on
699 Climate Change. Clouds and aerosols. In: Stocker, T. F., Qin, D., Plattner, G. K., Tignor, M., Allen,
700 S. K., Doschung, J., Nauels, A., Xia, Y., Bex, V., Midgley, P. M., Eds. *Climate change 2013: the*
701 *physical science basis*. Cambridge University Press, Cambridge, United Kingdom and New York,
702 616–617, 2013.

703 Bressi, M., Sciare, J., Gherzi, V., Bonnaire, N., Nicolas, J. B., Petit, J. E., Moukhtar, S., Rosso, A.,
704 and Féron, A.: A one-year comprehensive chemical characterisation of fine aerosol (PM_{2.5}) at urban,
705 suburban and rural background sites in the region of Paris (France), *Atmos. Chem. Phys.*, 13(15),
706 7825-7844, 2013.

707 Cao, J. J., Lee, S. C., Zhang, X. Y., Chow, J. C., An, Z. S., Ho, K. F., Watson, J. G., Fung, K., Wang,
708 Y. Q., and Shen, Z. X.: Characterization of airborne carbonate over a site near Asian dust source
709 regions during spring 2002 and its climatic and environmental significance, *J. Geophys. Res.:*
710 *Atmos.*, 110, doi:10.1029/2004JD005244, 2005.

711 Chang, Y., Deng, C., Cao, F., Cao, C., Zou, Z., Liu, S., Lee, X., Li, J., Zhang, G., and Zhang, Y.:
712 Assessment of carbonaceous aerosols in Shanghai, China – Part 1: long-term evolution, seasonal
713 variations, and meteorological effects, *Atmos. Chem. Phys.*, 17, 9945-9964,
714 <https://doi.org/10.5194/acp-17-9945-2017>, 2017.

715 Chen, D., Cui, H., Zhao, Y., Yin, L., Lu, Y., and Wang, Q.: A two-year study of carbonaceous
716 aerosols in ambient PM_{2.5} at a regional background site for western Yangtze River Delta, China,
717 *Atmos. Res.*, 183, 351-361, 2017.

718 **Chen, H. and Chen, W.: Potential impact of shifting coal to gas and electricity for building sectors**
719 **in 28 major northern cities of China. *Appl. Energ.*, 236, 1049-1061, 2019.**

720 Chen, X. C., Ward, T. J., Cao, J. J., Lee, S. C., Chow, J. C., Lau, G. N. C., Yim, S. H. L., and Ho, K.
721 F.: Determinants of personal exposure to fine particulate matter (PM_{2.5}) in adult subjects in Hong
722 Kong, *Sci. Total Environ.*, 628-629, 1165-1177, <https://doi.org/10.1016/j.scitotenv.2018.02.049>,

723 2018.

724 Chen, Y., Xie, S., Luo, B., and Zhai, C.: Characteristics and origins of carbonaceous aerosol in the
725 Sichuan Basin, China, *Atmos. Environ.*, 94, 215-223, 2014.

726 Chen, Y., Xie, S. D., Luo, B., and Zhai, C. Z.: Particulate pollution in urban Chongqing of southwest
727 China: Historical trends of variation, chemical characteristics and source apportionment, *Sci. Total*
728 *Environ.*, 584, 523-534, 2017

729 Cheng, N., Chen, Z., Sun, F., Sun, R., Dong, X., Xie, X., and Xu, C.: Ground ozone concentrations
730 over Beijing from 2004 to 2015: Variation patterns, indicative precursors and effects of emission
731 reduction, *Environ. Pollut.*, 237, 262-274, <https://doi.org/10.1016/j.envpol.2018.02.051>, 2018.

732 Chow, J. C., Watson, J. G., Lu, Z., Lowenthal, D. H., Frazier, C. A., Solomon, P. A., Thuillier, R. H.,
733 and Magliano, K.: Descriptive analysis of PM_{2.5} and PM₁₀ at regionally representative locations
734 during SJVAQS/AUSPEX, *Atmos. Environ.*, 30, 2079-2112, [https://doi.org/10.1016/1352-](https://doi.org/10.1016/1352-2310(95)00402-5)
735 [2310\(95\)00402-5](https://doi.org/10.1016/1352-2310(95)00402-5), 1996.

736 Dai, Q. L., Bi, X. H., Liu, B. S., Li, L. W., Ding, J., Song, W. B., Bi, S. Y., Schulze, B. C., Song, C.
737 B., Wu, J. H., Zhang, Y. F., Feng, Y. C., and Hopke, P. K.: Chemical nature of PM_{2.5} and PM₁₀ in
738 Xi'an, China: Insights into primary emissions and secondary particle formation, *Environ. Pollut.*
739 240, 155-166, 2018.

740 Dan, M., Zhuang, G., Li, X., Tao, H., and Zhuang, Y.: The characteristics of carbonaceous species
741 and their sources in PM_{2.5} in Beijing, *Atmos. Environ.*, 38, 3443-3452,
742 <https://doi.org/10.1016/j.atmosenv.2004.02.052>, 2004.

743 Ding, A. J., Huang, X., Nie, W., Sun, J. N., Kerminen, V. M., Petäjä, T., Su, H., Cheng, Y. F., Yang,
744 X. Q., Wang, M. H., Chi, X. G., Wang, J. P., Virkkula, A., Guo, W. D., Yuan, J., Wang, S. Y.,
745 Zhang, R. J., Wu, Y. F., Song, Y., Zhu, T., Zilitinkevich, S., Kulmala, M., and Fu, C. B.: Enhanced
746 haze pollution by black carbon in megacities in China, *Geophys. Res. Lett.*, 43, 2873–2879, 2016.

747 Duan, F., He, K., Ma, Y., Yang, F., Yu, X., Cadle, S., Chan, T., and Mulawa, P.: Concentration and
748 chemical characteristics of PM_{2.5} in Beijing, China: 2001–2002, *Sci. Total Environ.*, 355, 264-275,
749 2006.

750 Gao, J., Woodward, A., Vardoulakis, S., Kovats, S., Wilkinson, P., Li, L., Xu, L., Li, J., Yang, J., Li,
751 J., Cao, L., Liu, X., Wu, H., and Liu, Q.: Haze, public health and mitigation measures in China: A

752 review of the current evidence for further policy response, *Sci. Total Environ.*, 578, 148-157,
753 <https://doi.org/10.1016/j.scitotenv.2016.10.231>, 2017.

754 Giglio, L.: MODIS Collection 5 Active Fire Product User's Guide Version 2.5
755 http://earthdata.nasa.gov/files/MODIS_Fire_Users_Guide_2.5.pdf, 2013.

756 Grivas, G., Cheristanidis, S., and Chaloulakou, A.: Elemental and organic carbon in the urban
757 environment of Athens. Seasonal and diurnal variations and estimates of secondary organic carbon,
758 *Sci. Total Environ.*, 414, 535-545, 2012.

759 Hallquist, M., Wenger, J., Baltensperger, U., Rudich, Y., Simpson, D., Claeys, M., Dommen, J.,
760 Donahue, N. M., George, C., Goldstein, A. H., Hamilton, J. F., Herrmann, H., Hoffmann, T., Iinuma,
761 Y., Jang, M., Jenkin, M. E., Jimenez, J. L., Kiendler-Scharr, A., Maenhaut, W., McFiggans, G.,
762 Mentel, Th. F., Monod, A., Prevot, A. S. H., Seinfeld, J. H., Surratt, J. D., Szmigielski, R., and Wildt,
763 J.: The formation, properties and impact of secondary organic aerosol: current and emerging issues,
764 *Atmospheric Chemistry and Physics* 9(14), 5155-5236, 2009.

765 Hassler, B., McDonald, B. C., Frost, G. J., Borbon, A., Carslaw, D. C., Civerolo, K., Granier, C.,
766 Monks, P. S., Monks, S., Parrish, D. D., Pollack, I. B., Rosenlof, K. H., Ryerson, T. B.,
767 Schneidemesser, E., and Trainer, M.: Analysis of long-term observations of NO_x and CO in
768 megacities and application to constraining emissions inventories, *Geophys. Res. Lett.*, 43, 9920-
769 9930, doi:10.1002/2016GL069894, 2016.

770 He, K., Yang, F., Ma, Y., Zhang, Q., Yao, X., Chan, C. K., Cadle, S., Chan, T., and Mulawa, P.: The
771 characteristics of PM_{2.5} in Beijing, China, *Atmos. Environ.*, 35, 4959-4970,
772 [https://doi.org/10.1016/S1352-2310\(01\)00301-6](https://doi.org/10.1016/S1352-2310(01)00301-6), 2001.

773 He, K. B., Yang, F. M., Duan, F. K., Ma Y. L.: Atmospheric particulate matter and regional complex
774 pollution, Science Press, Beijing, China. 310-327, 2011.

775 Henry, R., Norris, G. A., Vedantham, R., and Turner, J. R.: Source region identification using
776 Kernel smoothing, *Environ. Sci. Technol.*, 43 (11), 4090-4097, [http://dx.doi.org/10.1021/](http://dx.doi.org/10.1021/es8011723)
777 [es8011723](http://dx.doi.org/10.1021/es8011723), 2009.

778 Hu, G., Sun, J., Zhang, Y., Shen, X., and Yang, Y.: Chemical composition of PM_{2.5} based on two-
779 year measurements at an urban site in Beijing. *Aerosol Air Qual. Res.*, 15, 1748-1759, 2015.

780 Huang, R. J., Zhang, Y. L., Bozzetti, C., Ho, K. F., Cao, J. J., Han, Y. M., Dällenbach, K. R., Slowik,
781 J. G., Platt, S. M., Canonaco, F., Zotter, P., Wolf, R., Pieber, S. M., Bruns, E. A., Crippa, M., Ciarelli,
782 G., Piazzalunga, A., Schwikowski, M., Abbaszade, G., Schnelle-Kreis, J., Zimmermann, R., An, Z.,
783 S., Szidat, S., Baltensperger, U., El Haddad, I., and Prévôt, A. S. H.: High secondary aerosol
784 contribution to particulate pollution during haze events in China, *Nature*, 514, 218-222, 2014.

785 Jeong, B., Bae, M. S., Ahn, J., and Lee, J.: A study of carbonaceous aerosols measurement in
786 metropolitan area performed during Korus-AQ 2016 campaign, *J. Kor. Soc. Atmos. Environ.*, 33,
787 2017.

788 Ji, D., Li, L., Wang, Y., Zhang, J., Cheng, M., Sun, Y., Liu, Z. R., Wang, L. L., Tang, G. Q., Hu, B.,
789 Chao, N., Wen, T. X., and Miao, H. Y.: The heaviest particulate air-pollution episodes occurred in
790 northern China in January, 2013: Insights gained from observation, *Atmos. Environ.*, 92, 546-556,
791 2014.

792 Ji, D. S., Wang, Y. S., Wang, L. L., Chen, L. F., Hu, B., Tang, G. Q., Xin, J. Y., Song, T., Wen, T. X.,
793 Sun, Y., Pan, Y. P., and Liu, Z. R.: Analysis of heavy pollution episodes in selected cities of northern
794 China, *Atmos. Environ.*, 50, 338-348, 2012.

795 Ji, D. S., Zhang, J. K., He, J., Wang, X. J., Pang, B., Liu, Z. R., Wang, L. L., and Wang, Y. S.:
796 Characteristics of atmospheric organic and elemental carbon aerosols in urban Beijing, China,
797 *Atmos. Environ.*, 125, 293-306, 2016.

798 Ji, D. S., Yan, Y. C., Wang, Z. S., He, J., Liu, B., Sun, Y., Gao, M., Li, Y., Cao, W., Cui, Y., Hu, B.,
799 Xin, J. Y., Wang, L. L., Liu, Z. R., Tang, G. Q., and Wang, Y. S.: Two-year continuous measurements
800 of carbonaceous aerosols in urban Beijing, China: Temporal variations, characteristics and source
801 analyses, *Chemosphere*, 200, 191-200, 2018.

802 Ji, D. S., Gao, M., Maenhaut, W., He, J., Wu, C., Cheng, L. J., Gao, W. K., Sun, Y., Sun, J. R., Xin,
803 J. Y., Wang, L. L., and Wang, Y. S.: The carbonaceous aerosol levels still remain a challenge in the
804 Beijing-Tianjin-Hebei region of China: Insights from continuous high temporal resolution
805 measurements in multiple cities, *Environ. Int.*, 126: 171-183, 2019.

806 Jin, Y., Andersson, H., and Zhang, S.: Air pollution control policies in China: a retrospective and
807 prospects, *Int. J. Env. Res. Pub. He.*, 13(12), 1219, 2016.

808 Lang, J., Zhang, Y., Zhou, Y., Cheng, S., Chen, D., Guo, X., Chen, S., Li, X. X., Xing, X. F., and

809 Wang, H. Y.: Trends of PM_{2.5} and chemical composition in Beijing, 2000-2015, *Aerosol Air Qual.*
810 *Res.*, 17, 412-425, 2017.

811 Li, B., Zhang, J., Zhao, Y., Yuan, S., Zhao, Q., Shen, G., and Wu, H.: Seasonal variation of urban
812 carbonaceous aerosols in a typical city Nanjing in Yangtze River Delta, China, *Atmos. Environ.*,
813 106, 223-231, 2015.

814 Li, C., Chen, P., Kang, S., Yan, F., Hu, Z., Qu, B., and Sillanpää, M.: Concentrations and light
815 absorption characteristics of carbonaceous aerosol in PM_{2.5} and PM₁₀ of Lhasa city, the Tibetan
816 Plateau, *Atmos. Environ.*, 127, 340-346, <https://doi.org/10.1016/j.atmosenv.2015.12.059>, 2016.

817 Li, C., McLinden, C., Fioletov, V., Krotkov, N., Carn, S., Joiner, J., Streets, D., He, H., Ren, X., Li,
818 Z., and Dickerson, R.: India is overtaking China as the world's largest emitter of anthropogenic
819 sulfur dioxide, *Scientific Reports*, DOI:10.1038/s41598-017-14639-8, 2017.

820 Li, Y. C., Shu, M., Ho, S. S. H., Yu, J. Z., Yuan, Z. B., Liu, Z. F., Wang, X. X., and Zhao, X. Q.:
821 Effects of chemical composition of PM_{2.5} on visibility in a semi-rural city of Sichuan Basin, *Aerosol*
822 *and Air Qual. Res.*, 18(4): 957-968, 2018.

823 Liang, Q., Jaeglé, L., Jaffe, D. A., Weiss-Penzias, P., Heckman, A., and Snow, J. A.: Long-range
824 transport of Asian pollution to the northeast Pacific: Seasonal variations and transport pathways of
825 carbon monoxide, *J. Geophys. Res-Atmos.*, 109, doi:10.1029/2003JD004402, 2004.

826 Liu, D., Li, J., Zhang, Y., Xu, Y., Liu, X., Ding, P., Shen, C., Chen, Y., Tian, C., and Zhang, G.: The
827 use of levoglucosan and radiocarbon for source apportionment of PM_{2.5} carbonaceous aerosols at a
828 background site in east China, *Environ. Sci. Technol.*, 47, 10454, 2013.

829 Liu, F., Zhang, Q., Tong, D., Zheng, B., Li, M., Huo, H., and He, K. B.: High-resolution inventory
830 of technologies, activities, and emissions of coal-fired power plants in China from 1990 to 2010,
831 *Atmos. Chem. Phys.*, 15, 13299-13317, <https://doi.org/10.5194/acp-15-13299-2015>, 2015.

832 Liu, G., Li, J., Wu, D., and Xu, H.: Chemical composition and source apportionment of the ambient
833 PM_{2.5} in Hangzhou, China, *Particuology*, 18, 135-143, 2015.

834 Lupu A. and Maenhaut, W.: Application and comparison of two statistical trajectory techniques for
835 identification of source regions of atmospheric aerosol species, *Atmos. Environ.*, 36, 5607-5618,
836 2002.

837 Lv, B., Zhang, B., and Bai, Y.: A systematic analysis of PM_{2.5} in Beijing and its sources from 2000
838 to 2012. *Atmos. Environ.*, 124, 98-108, 2016.

839 Malm, W. C., Sisler, J. F., Huffman, D., Eldred, R. A., and Cahill, T. A.: Spatial and seasonal trends
840 in particle concentration and optical extinction in the United States, *J. Geophys. Res-Atmos.*, 99,
841 1347-1370, doi:10.1029/93JD02916, 1994.

842 Miyakawa, T., Kanaya, Y., Komazaki, Y., Miyoshi, T., Nara, H., Takami, A., Moteki, N., Koike, M.,
843 and Kondo, Y.: Emission regulations qltered the concentrations, origin, and formation of
844 carbonaceous aerosols in the Tokyo metropolitan area, *Aerosol Air Qual. Res.*, 16, 1603-1614,
845 10.4209/aaqr.2015.11.0624, 2016.

846 Na, K., Sawant, A. A., Song, C., and Cocker, D. R.: Primary and secondary carbonaceous species
847 in the atmosphere of Western Riverside County, California, *Atmos. Environ.*, 38, 1345-1355,
848 <https://doi.org/10.1016/j.atmosenv.2003.11.023>, 2004.

849 Niu, X. Y., Cao, J. J., Shen, Z. X., Ho, S. S. H., Tie, X. X., Zhao, S. Y., Xue, H. M., Zhang, T., and
850 Huang, R. J.: PM_{2.5} from the Guanzhong Plain: Chemical composition and implications for emission
851 reductions, *Atmos. Environ.*, 147, 458-469, 2016.

852 Paraskevopoulou, D., Liakakou, E., Gerasopoulos, E., Theodosi, C., and Mihalopoulos, N.: Long-
853 term characterization of organic and elemental carbon in the PM_{2.5} fraction: the case of Athens,
854 Greece, *Atmos. Chem. Phys.*, 14(23), 13313-13325, 2014.

855 Park, J. S., Song, I. H., Park, S. M., Shin, H., and Hong, Y.: The characteristics and seasonal
856 variations of OC and EC for PM_{2.5} in Seoul metropolitan area in 2014, *J. Environ. Impact Assess.*,
857 24, 578-592, 2015.

858 Peltier, R. E., Weber, R. J., and Sullivan, A. P.: Investigating a liquid-based method for online
859 organic carbon detection in atmospheric particles, *Aerosol Sci. Tech.*, 41, 1117-1127,
860 10.1080/02786820701777465, 2007.

861 Pereira, G. M., Teinilä, K., Custódio, D., Santos, A. G., Xian, H., Hillamo, R., Alves, C. A., Andrade,
862 J. B., Rocha, G. O., Kumar, P., Balasubramanian, R., Andrade M. F., and Vasconcellos, P. C.:
863 Airborne particles in the Brazilian city of São Paulo: One-year investigation for the chemical
864 composition and source apportionment, *Atmos. Chem. Phys.*, 17, 11943-11969, 2017.

865 Petit, J. E., Favez, O., Albinet, A., and Canonaco, F.: A user-friendly tool for comprehensive

866 evaluation of the geographical origins of atmospheric pollution: Wind and trajectory analyses.
867 Environ. Modell. Softw., 88, 183-187, 2017.

868 Poirot, R. L. and Wishinski, P. R.: Visibility, sulfate and air mass history associated with the
869 summertime aerosol in northern Vermont, Atmos. Environ., 20, 1457-1469, 1986.

870 Polissar, A. V., Hopke, P. K., and Harris, J. M.: Source regions for atmospheric aerosol measured at
871 Barrow, Alaska, Environ. Sci. Technol., 35, 4214-4226, 2001.

872 Ram, K. and Sarin, M. M.: Spatio-temporal variability in atmospheric abundances of EC, OC and
873 WSOC over Northern India, J. Aerosol Sci., 41, 88-98,
874 <https://doi.org/10.1016/j.jaerosci.2009.11.004>, 2010.

875 Ram, K. and Sarin, M.: Carbonaceous aerosols over Northern India: sources and spatio-temporal
876 variability, Proc. Indian Natn. Sci. Acad., 78, 523-533, 2012.

877 Ren, Z. H., Wan, B. T., Yu, T., Su, F. Q., Zhang, Z. G., Gao, Yang, X. X., Hu, H. L., Wu, Y. H., Hu,
878 F., and Hong, Z. X.: Influence of weather system of different scales on pollution boundary layer and
879 the transport in horizontal current field, Res. Environ. Sci., 17(1), 7-13, 2004.

880 Rollins, A. W., Browne, E. C., Min, K. E., Pusede, S. E., Wooldridge, P. J., Gentner, D. R., Goldstein,
881 A. H., Liu, S., Day, D. A., Russell, L. M., and Cohen, R. C.: Evidence for NO_x control over
882 nighttime SOA formation, Science 337(6099), 1210-1212, 2012.

883 Schauer, J. J., Kleeman, M. J., Cass, G. R., and Simoneit, B. R.: Measurement of emissions from
884 air pollution sources. 5. C1-C32 organic compounds from gasoline-powered motor vehicles,
885 Environ. Sci. Technol., 36, 1169–1180, 2002.

886 Seinfeld, J. H. and Pandis, S. N.: Atmospheric chemistry and physics: from air pollution to climate
887 change, John Wiley & Sons, 1998.

888 Shah, J. J., Johnson, R. L., Heyerdahl, E. K., and Huntzicker, J. J.: Carbonaceous aerosol at urban
889 and rural sites in the United States, J. Air Pollut. Control Assoc., 36, 254-257, 1986.

890 Sharma, S. K. and Mandal, T. K.: Chemical composition of fine mode particulate matter (PM_{2.5}) in
891 an urban area of Delhi, India and its source apportionment, Urban Clim., 21, 106-122,
892 <https://doi.org/10.1016/j.uclim.2017.05.009>, 2017.

893 Shi, G. L., Peng, X., Liu, J. Y., Tian, Y. Z., Song, D. L., Yu, H. F., Feng, Y. C., and Russell, A. G.:
894 Quantification of long-term primary and secondary source contributions to carbonaceous aerosols,

895 Environ. Pollut. 219, 897-905, 2016.

896 Sofowote, U. M., Rastogi, A. K., Deboz, J., and Hopke, P. K.: Advanced receptor modeling of
897 near-real-time, ambient PM_{2.5} and its associated components collected at an urban-industrial site
898 in Toronto, Ontario, Atmos. Pollut. Res., 5, 13-23, <https://doi.org/10.5094/APR.2014.003>, 2014.

899 Song, Y., Xie, S., Zhang, Y., Zeng, L., Salmon, L. G., and Zheng, M.: Source apportionment of
900 PM_{2.5} in Beijing using principal component analysis/absolute principal component scores and
901 UNMIX, Sci. Total Environ., 372, 278-286, 2006.

902 Tang, G., Zhang, J., Zhu, X., Song, T., Munkel, C., Hu, B., Schäfer, K., Liu, Z., Zhang, J., Wang,
903 L., Xin, J., Suppan, P., and Wang, Y.: Mixing layer height and its implications for air pollution over
904 Beijing, China, Atmos. Chem. Phys., 16, 2459-2475, <https://doi.org/10.5194/acp-16-2459-2016>,
905 2016.

906 Tao, J., Cheng, T., Zhang, R., Cao, J., Zhu, L., Wang, Q., Luo, L., and Zhang, L.: Chemical
907 composition of PM_{2.5} at an urban site of Chengdu in southwestern China, Adv. Atmos. Sci., 30,
908 1070-1084, 2013.

909 Tao, J., Gao, J., Zhang, L., Zhang, R., Che, H., Zhang, Z., Lin, Z., Jing, J., Cao, J., and Hsu, S. C.:
910 PM_{2.5} pollution in a megacity of southwest China: source apportionment and implication, Atmos.
911 Chem. Phys., 14, 2014.

912 Tao, J., Zhang, L., Cao, J., and Zhang, R.: A review of current knowledge concerning PM_{2.5}
913 chemical composition, aerosol optical properties and their relationships across China, Atmos. Chem.
914 Phys., 17(15), 9485-9518, 2017.

915 Villalobos, A. M., Amonov, M. O., Shafer, M. M., Devi, J. J., Gupta, T., Tripathi, S. N., Rana, K. S.,
916 McKenzie, M., Bergin, M. H., and Schauer, J. J.: Source apportionment of carbonaceous fine
917 particulate matter (PM_{2.5}) in two contrasting cities across the Indo-Gangetic Plain, Atmos. Pollut.
918 Res., 6, 398-405, <https://doi.org/10.5094/APR.2015.044>, 2015.

919 Wang, C., An, X., Zhang, P., Sun, Z., Cui, M., and Ma, L.: Comparing the impact of strong and
920 weak East Asian winter monsoon on PM_{2.5} concentration in Beijing, Atmos. Res., 215, 165-177,
921 2019.

922 Wang, J., Allen, D. J., Pickering, K. E., Li, Z., and He, H.: Impact of aerosol direct effect on East
923 Asian air quality during the EAST - AIRE campaign, *J. Geophys. Res-Atmos.*, 121(11), 6534-6554,
924 2016b.

925 Wang, L., Zhou, X., Ma, Y., Cao, Z., Wu, R., and Wang, W.: Carbonaceous aerosols over China-
926 review of observations, emissions, and climate forcing, *Environ. Sci. Pollut. Res.*, 23(2), 1671-1680,
927 2016a.

928 Wang, P., Cao, J. J., Shen, Z. X., Han, Y. M., Lee, S. C., Huang, Y., Zhu, C. S., Wang, Q. Y., Xu, H.
929 M., and Huang, R. J.: Spatial and seasonal variations of PM_{2.5} mass and species during 2010 in Xi'an,
930 China, *Sci. Total Environ.*, 508, 477-487, <https://doi.org/10.1016/j.scitotenv.2014.11.007>, 2015.

931 Wang, Y., Khalizov, A., Levy, M., and Zhang, R. Y.: New Directions: light absorbing aerosols and
932 their atmospheric impacts, *Atmos. Environ.*, 81, 713–715, 2013.

933 Wang, Y. Q., Zhang, X. Y., and Draxler, R. R.: TrajStat: GIS-based software that uses various
934 trajectory statistical analysis methods to identify potential sources from long-term air pollution
935 measurement data, *Environ. Modell. Softw.*, 24(8), 938-939, 2009.

936 Wang, Z. S., Zhang, D. W., Liu, B. X., Li, Y. T., Chen, T., Sun, F., Yang, D. Y., Liang, Y. P., Chang,
937 M., Liu, Y., and Lin, A. G.: Analysis of chemical characteristics of PM_{2.5} in Beijing over a 1-year
938 period, *J. Atmos. Chem.*, 73(4): 407-425, 2016c.

939 WHO. Health effects of black carbon. <http://wedocs.unep.org/handle/20.500.11822/8699>, 2012.

940 Wood, E. C., Canagaratna, M. R., Herndon, S. C., Onasch, T. B., Kolb, C. E., Worsnop, D. R., Kroll,
941 J. H., Knighton, W. B., Seila, R., Zavala, M., Molina, L. T., DeCarlo, P. F., Jimenez, J. L.,
942 Weinheimer, A. J., Knapp, D. J., Jobson, B. T., Stutz, J., Kuster, W. C., Williams, E. J.: Investigation
943 of the correlation between odd oxygen and secondary organic aerosol in Mexico City and Houston.
944 *Atmos. Chem. Phys.* 18(10), 8947-8968, 2010.

945 Wu, C., Wu, D., and Yu, J. Z.: Quantifying black carbon light absorption enhancement with a novel
946 statistical approach, *Atmos. Chem. Phys.*, 18, 289-309, <https://doi.org/10.5194/acp-18-289-2018>,
947 2018.

948 Wu, D., Liao B. T, Wu M., Chen, H., Wang, Y., Niao, X., Gu, Y., Zhang, X., Zhao, X. J., Quan, J.
949 N., Liu, W. D., Meng, J., and Sun, D.: The long-term trend of haze and fog days and the surface
950 layer transport conditions under haze weather in North China, *Acta Sci Circumst.*, 34, 1-11, 2014.

951 Wu, H., Zhang, Y. F., Han, S. Q., Wu, J. H., Bi, X. H., Shi, G. L., Wang, J., Yao, Q., Cai, Z. Y., Liu,
952 J. L., and Feng, Y. C.: Vertical characteristics of PM_{2.5} during the heating season in Tianjin, China,
953 *Sci. Total Environ.*, 523, 152-160, <https://doi.org/10.1016/j.scitotenv.2015.03.119>, 2015.

954 Wu, X., Wu, Y., Zhang, S., Liu, H., Fu, L., and Hao, J.: Assessment of vehicle emission programs
955 in China during 1998–2013: achievement, challenges and implications, *Environ. Pollut.*, 214, 556-
956 567, 2016.

957 Xing, J., Wang, J., Mathur, R., Wang, S., Sarwar, G., Pleim, J., Hogrefe, C., Zhang, Y., Jiang, J.,
958 Wong, D. C., and Hao, J.: Impacts of aerosol direct effects on tropospheric ozone through changes
959 in atmospheric dynamics and photolysis rates, *Atmos. Chem. Phys.*, 17, 9869-9883, 2017.

960 Xu, J., Wang, Q., Deng, C., McNeill, V. F., Fankhauser, A., Wang, F., Zheng, X., Shen, J., Huang,
961 K., and Zhuang, G.: Insights into the characteristics and sources of primary and secondary organic
962 carbon: High time resolution observation in urban Shanghai, *Environ. Pollut.*, 233, 1177-1187,
963 <https://doi.org/10.1016/j.envpol.2017.10.003>, 2018.

964 Yang, F., He, K., Ye, B., Chen, X., Cha, L., Cadle, S.H., Chan, T., and Mulawa, P. A.: One-year
965 record of organic and elemental carbon in fine particles in downtown Beijing and Shanghai, *Atmos.*
966 *Chem. Phys.*, 5, 1449–1457, 2005.

967 Yang, F., Huang, L., Duan, F., Zhang, W., He, K., Ma, Y., Brook, J. R., Tan, J., Zhao, Q., and Cheng,
968 Y.: Carbonaceous species in PM_{2.5} at a pair of rural/urban sites in Beijing, 2005-2008, *Atmos. Chem.*
969 *Phys.*, 11, 7893–7903, 2011a.

970 Yang, F., Tan, J., Zhao, Q., Du, Z., He, K., Ma, Y., Duan, F., and Chen, G.: Characteristics of PM_{2.5}
971 speciation in representative megacities and across China, *Atmos. Chem. Phys.*, 11, 5207-5219,
972 2011b.

973 Yi, K., Liu, J. F., Wang, X. J., Ma, J. M., Hu, J. Y., Wan, Y., Xu, J. Y., Yang H. Z., Liu, H. Z.,
974 Xiang, S. L., and Tao, S.: A combined Arctic-tropical climate pattern controlling the inter-annual
975 climate variability of wintertime PM_{2.5} over the North China Plain. *Environ. Pollut.*, 245, 607-615,
976 2019.

977 Yu, X. Y., Cary, R. A., and Laulainen, N. S.: Primary and secondary organic carbon downwind of
978 Mexico City, *Atmos. Chem. Phys.*, 9(18), 6793-6814, 2009.

979 Zhang, F., Zhao, J., Chen, J., Xu, Y., and Xu, L.: Pollution characteristics of organic and elemental

980 carbon in PM_{2.5} in Xiamen, China, *J. Environ. Sci.*, 23(8), 1342-1349, 2011.

981 Zhang, F., Wang, Z. W., Cheng, H. R., Lv, X. P., Gong, W., Wang, X. M., and Zhang, G.: Seasonal
982 variations and chemical characteristics of PM_{2.5} in Wuhan, central China, *Sci. Total Environ.*, 518-
983 519, 97-105, <https://doi.org/10.1016/j.scitotenv.2015.02.054>, 2015.

984 Zhang, R., Jing, J., Tao, J., Hsu, S. C., Wang, G., Cao, J., Lee, C. S. L., Zhu, L., Chen, Z., Zhao, Y.,
985 and Shen Z.: Chemical characterization and source apportionment of PM_{2.5} in Beijing: seasonal
986 perspective, *Atmos. Chem. Phys.*, 13, 7053–7074, 2013.

987 Zhang, R. Y., Khalizov, A. F., Pagels, J., Zhang, D., Xue, H., and McMurry, P. H.: Variability in
988 morphology, hygroscopicity, and optical properties of soot aerosols during atmospheric processing,
989 *Proc. Natl. Acad. Sci. U.S.A.*, 105, 10291–10296, 2008.

990 Zhang, Y., Li, C., Krotkov, N. A., Joiner, J., Fioletov, V., and McLinden, C.: Continuation of long-
991 term global SO₂ pollution monitoring from OMI to OMPS, *Atmos. Meas. Tech.*, 10, 1495-1509,
992 <https://doi.org/10.5194/amt-10-1495-2017>, 2017.

993 Zhang, Y., Zhang, Q., Cheng, Y., Su, H., Li, H., Li, M., Zhang, X., Ding, A., and He, K.:
994 Amplification of light absorption of black carbon associated with air pollution, *Atmos. Chem. Phys.*,
995 18, 9879-9896, <https://doi.org/10.5194/acp-18-9879-2018>, 2018.

996 Zhao, M., Huang, Z., Qiao, T., Zhang, Y., Xiu, G., and Yu, J.: Chemical characterization, the
997 transport pathways and potential sources of PM_{2.5} in Shanghai: Seasonal variations, *Atmos. Res.*,
998 158, 66-78, 2015a.

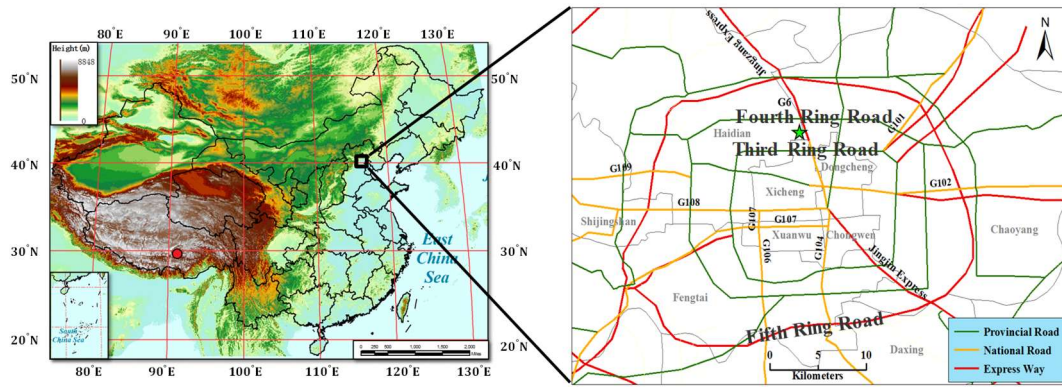
999 Zhao, M., Qiao, T., Huang, Z., Zhu, M., Xu, W., Xiu, G., Tao, J., and Lee, S.: Comparison of ionic
1000 and carbonaceous compositions of PM_{2.5} in 2009 and 2012 in Shanghai, China, *Sci. Total Environ.*,
1001 536, 695-703, 2015b.

1002 **Zhao, P., Dong, F., and Yang, Y.: Characteristics of carbonaceous aerosol in the region of Beijing,**
1003 **Tianjin, and Hebei, China, *Atmos. Environ.*, 71, 389-398, 2013.**

1004 Zheng, B., Tong, D., Li, M., Liu, F., Hong, C., Geng, G., Li, H. Y., Li, X., Peng, L. Q., Qi, J., Yan,
1005 L., Zhang, Y. X., Zhao, H. Y., Zheng, Y. X., He, K. B., and Zhang, Q.: Trends in China's
1006 anthropogenic emissions since 2010 as the consequence of clean air actions, *Atmos. Chem. Phys.*,
1007 18, 14095–14111, 2018.

1008 Zhu, C., Tian, H., Hao, Y., Gao, J., Hao, J., Wang, Y., Hua, S., Wang, K., and Liu, H.: A high-resolution

1009 emission inventory of anthropogenic trace elements in Beijing-Tianjin-Hebei (BTH) region of China,
1010 Atmos. Environ., 191, 452-462, <https://doi.org/10.1016/j.atmosenv.2018.08.035>, 2018.
1011

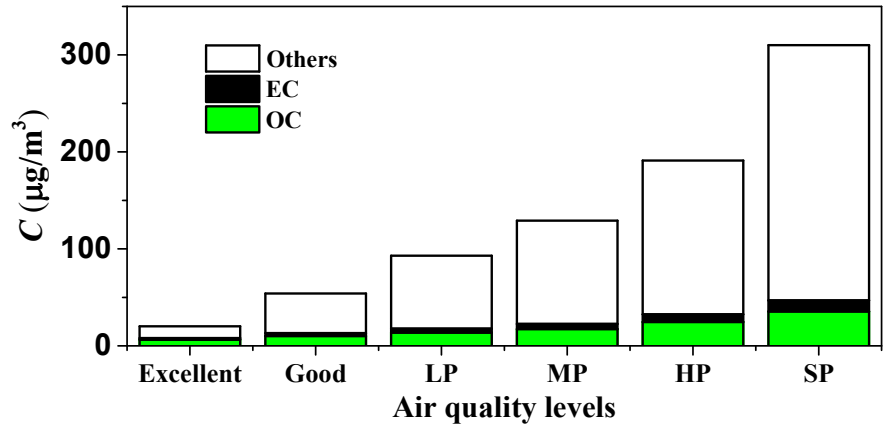


G6=Jingzang Expressway; G101=National Highway 101; G102= National Highway 102;
 G107= National Highway 107; G108= National Highway 108; G109= National Highway 109

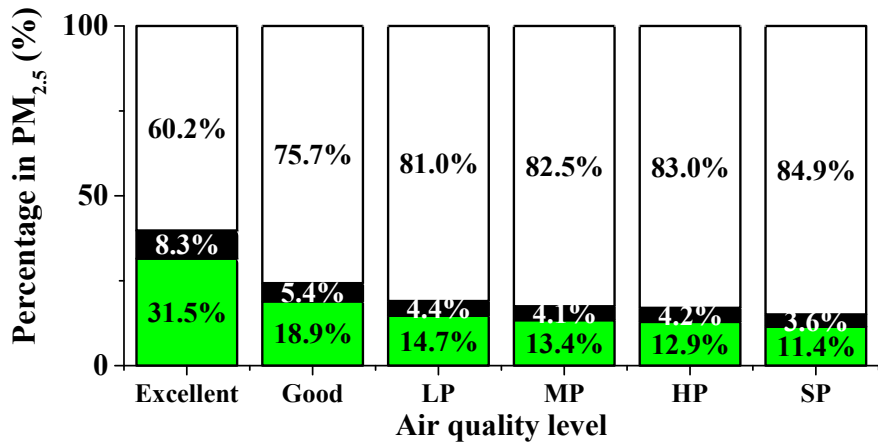
1012

1013 Fig. 1. Map with location of the sampling site (the asterisk in the right figure indicates the sampling
 1014 site).

1015



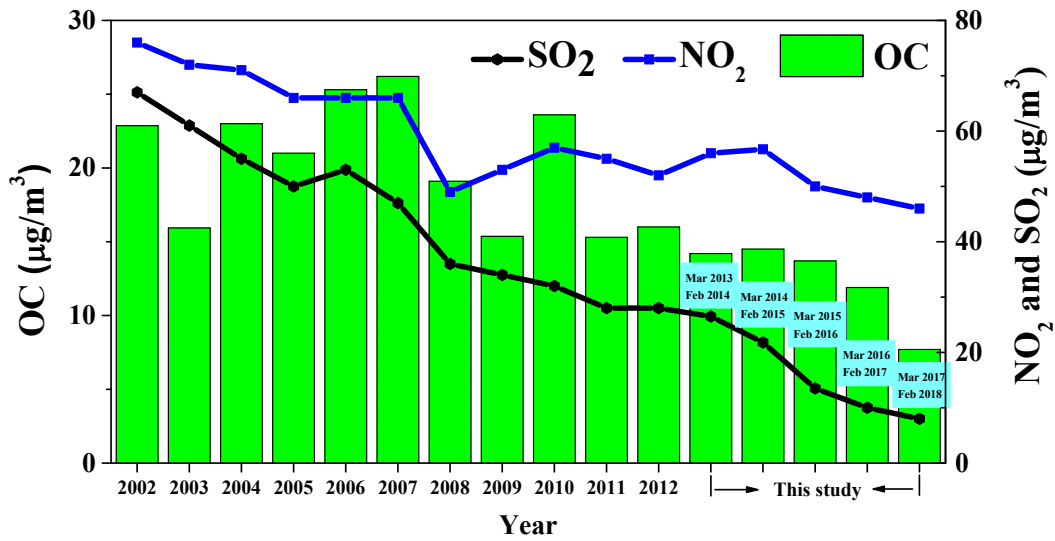
1016



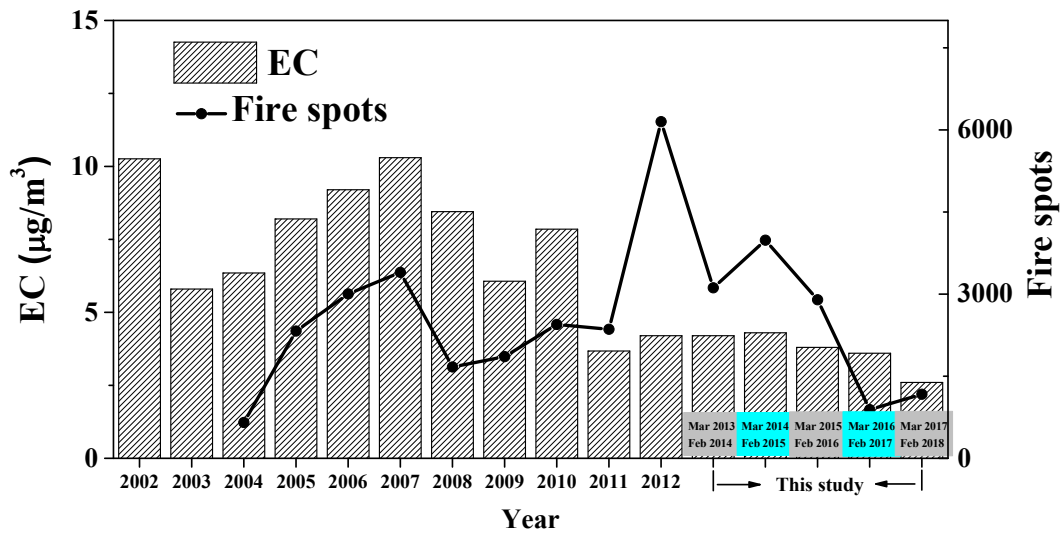
1017

1018 Fig. 2. Variation of average OC, EC and PM_{2.5} concentrations (top) and of the percentages of OC,
 1019 EC and other components in PM_{2.5} (bottom) for different air quality levels.

1020



1021



1022

1023 Fig. 3. Variation of the annual mean OC and EC concentrations in PM_{2.5} from 2002 to
 1024 2018 in Beijing. The variation in NO₂ and SO₂ concentrations and in the number of fire
 1025 spots counted for the domain of (30-70° N, 65-150° E) is also shown.

1026

1027

1028

1029

1030

1031

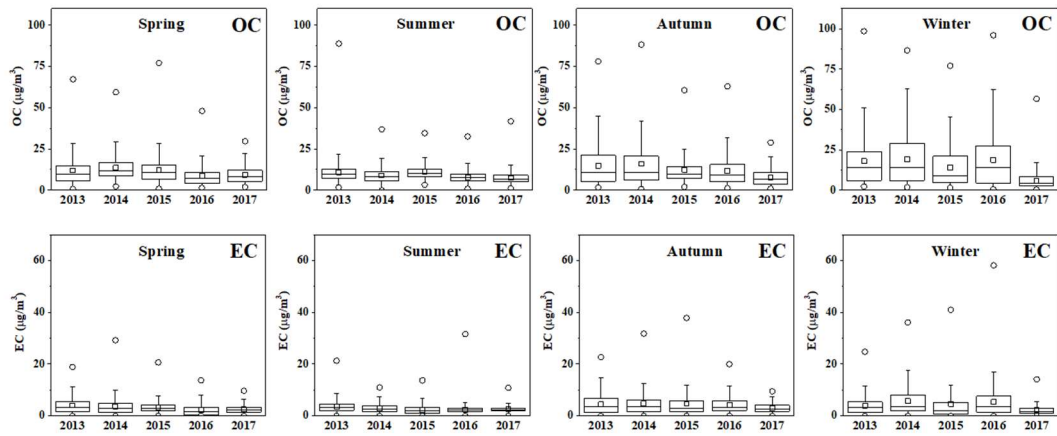
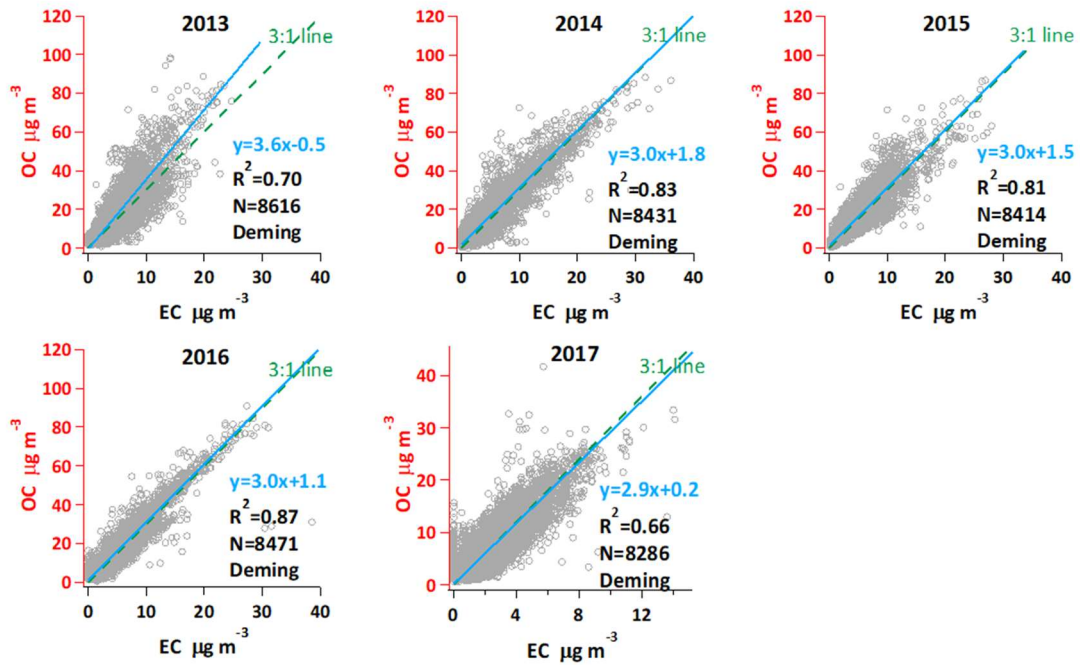


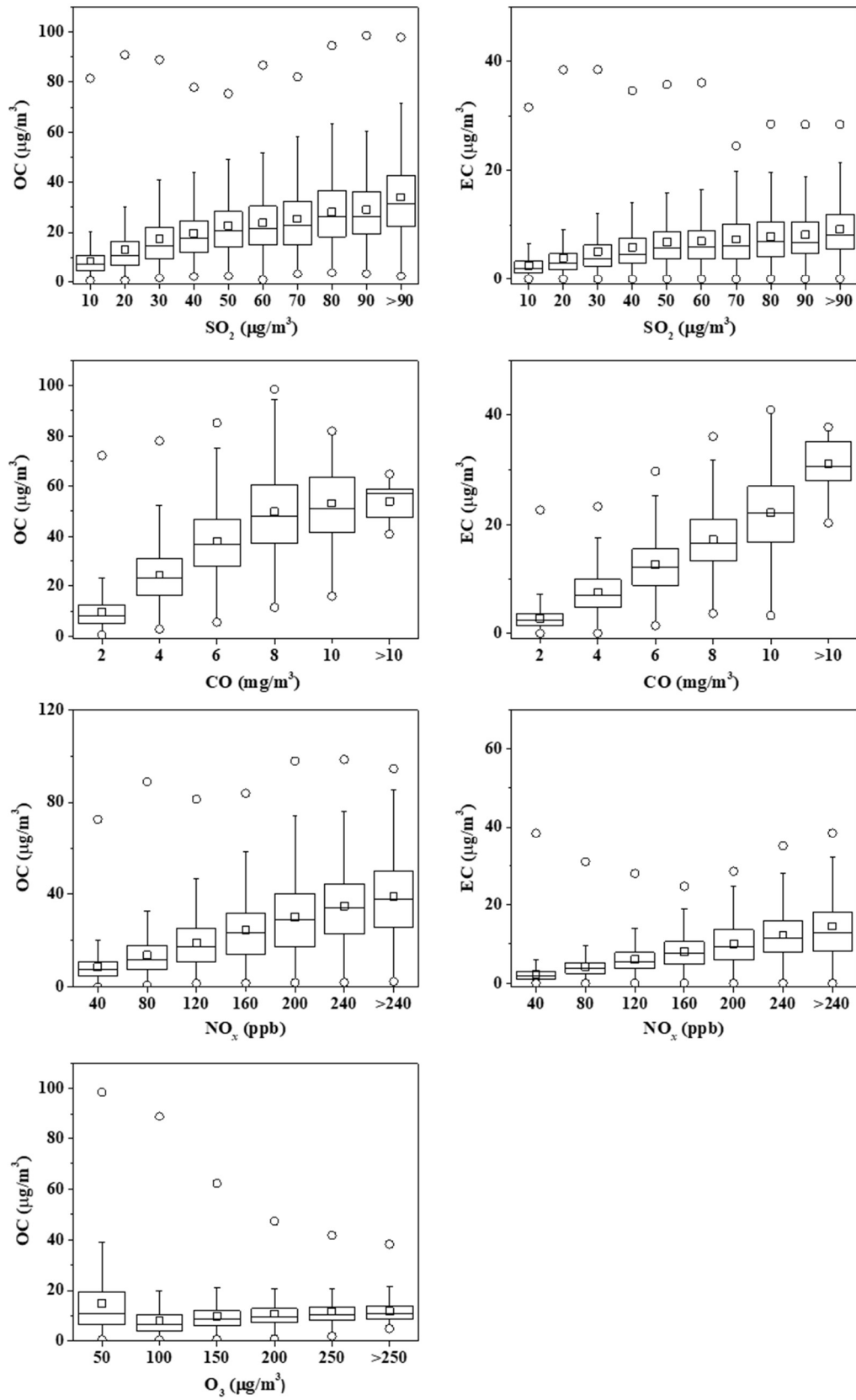
Fig. 4. Seasonal variations of OC and EC concentrations from March 2013 to February 2018.



1032

1033 Fig. 5. Relationship between OC and EC using the Deming regression method from 2013 to 2017
 1034 (the dashed line indicates a OC/EC ratio of 3:1).

1035

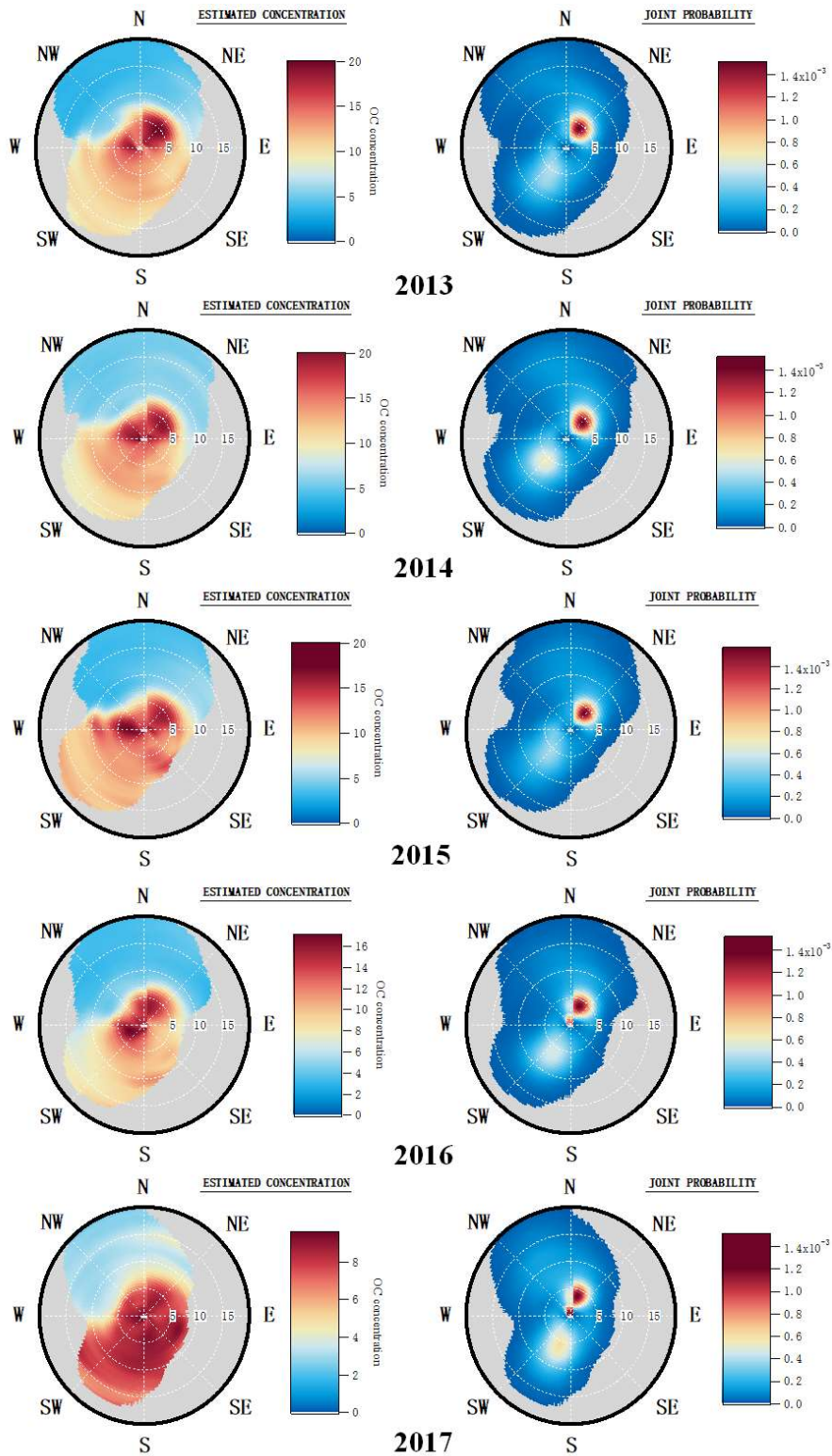


1036

1037

Fig. 6. OC and EC concentrations as a function of the SO₂, CO, NO_x and O₃ concentration.

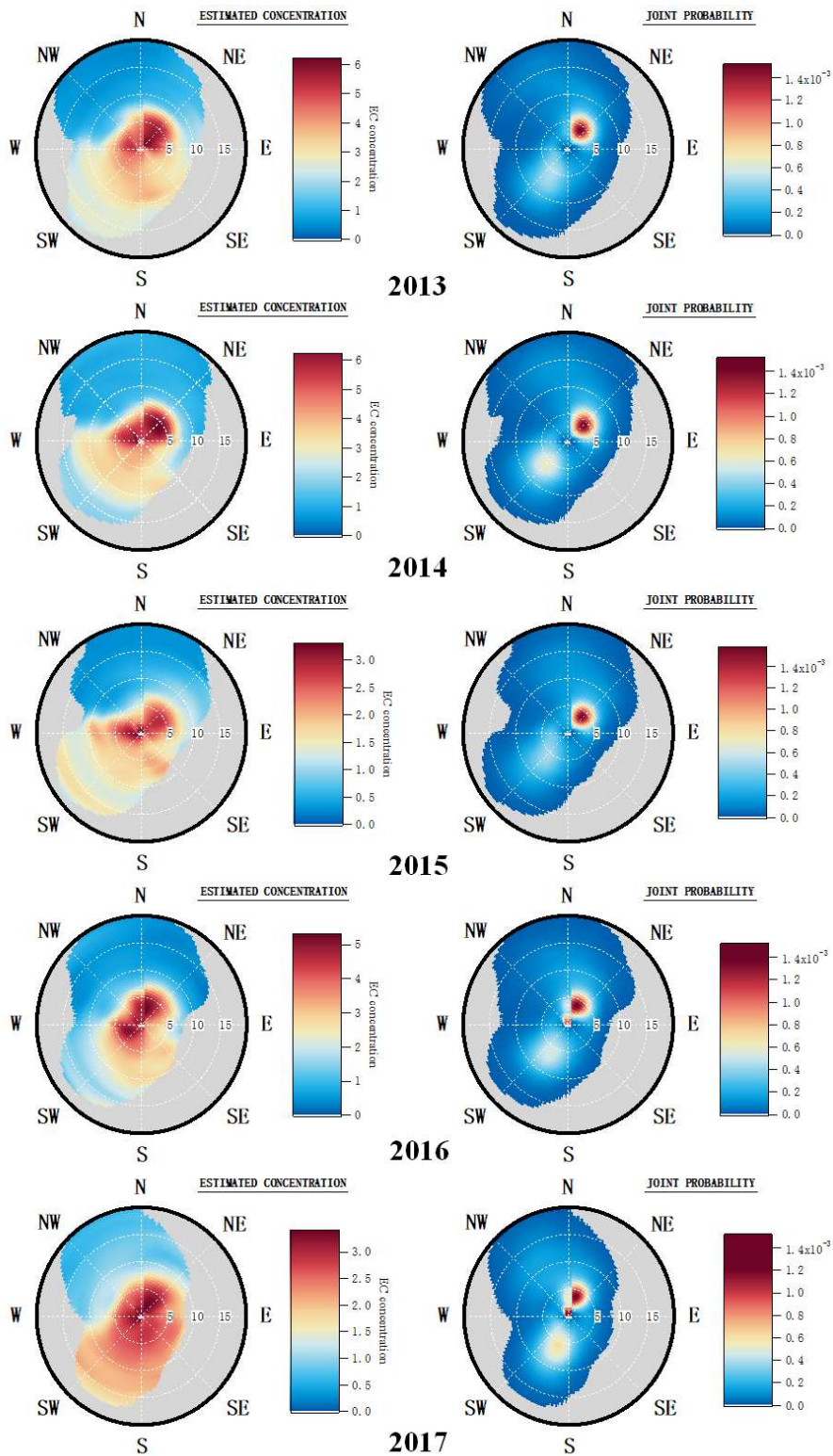
1038



1039

1040 Fig. 7. Wind analysis results using NWR on 1-h OC concentrations measured in Beijing from 2013
 1041 to 2017 (Unit of wind speed: km/h).

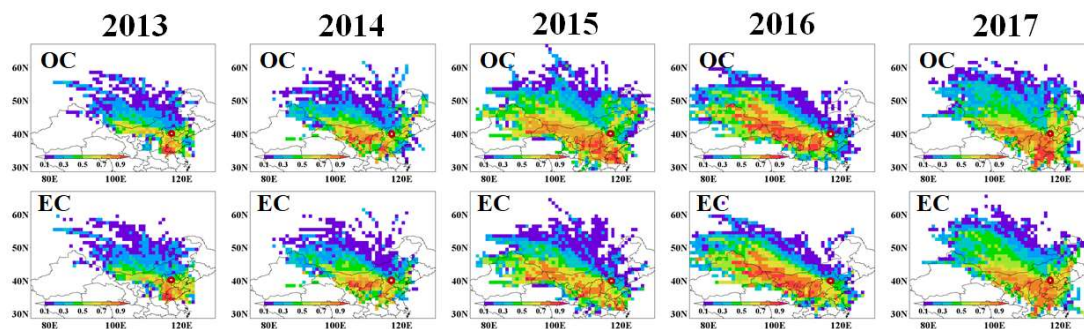
1042




1043

1044 Fig. 8. Wind analysis results using NWR on 1-h EC concentrations measured in Beijing from 2013
 1045 to 2017.

1046



1047

1048 Fig. 9 Potential source areas for OC and EC in Beijing from 2013 to 2017. The color code denotes
 1049 the PSCF probability. The measurement site is indicated with a . The identification of the
 1050 provinces is given in Fig. S9.

1051

1052 Table 1. Medians, averages and associated standard deviations for the OC, EC and PM_{2.5} concentrations (in µg/m³) and averages for the OC/PM_{2.5}, EC/PM_{2.5} and
 1053 TC/PM_{2.5} ratios from March 2013 to February 2018.

	OC			EC			PM _{2.5}			OC/PM _{2.5}	EC/PM _{2.5}	TC/PM _{2.5}
	Median	Average	Stdev	Median	Average	Stdev	Median	Average	Stdev	Average	Average	Average
Mar-2013 – Feb-2014	10.6	14	11.7	3.2	4	3.3	66	89	82.9	0.157	0.045	0.203
Mar-2014 – Feb-2015	10.4	14.5	12.1	3	4.3	4	66	85.5	76.6	0.169	0.05	0.219
Mar-2015 – Feb-2016	9.1	13.7	9.2	1.3	3.8	4.4	48	76.9	85.6	0.178	0.049	0.228
Mar-2016 – Feb-2017	8.2	11.9	11.3	2.5	3.6	3.7	53	79.4	82.8	0.15	0.045	0.195
Mar-2017 – Feb-2018	6.8	7.7	4.7	2.3	2.6	1.6	35	49.4	48.6	0.155	0.052	0.208
whole study period	9.3	12.4	10.6	2.7	3.7	3.6	52	75.7	77.6	0.164	0.049	0.213

1054

1055 Table 2. Mean or median OC and EC mass concentrations (in $\mu\text{g}/\text{m}^3$) observed in major megacities of the world published in the literature and obtained in this study.

1056

1057

Megacities	Method	Period	Number or frequency of sampling	OC	EC	Literature
Athens	TOT	May 2008 to April 2013	Once everyday	2.1	0.54	Paraskevopoulou et al., 2014
Beijing	TOT	March 2017-February 2018	Hourly	7.7	2.6	This study
Hongkong	TOR	from July to October 2014 and December 2014 to March 2015	N=161	7.8	2.2	Chen et al., 2018
Lhasa	TOR	May 2013 to March 2014	once each week	3.27	2.24	Li et al., 2016
Los Angeles	TOT	March 2017-February 2018	once every 3 days	2.88	0.56	US EPA*
Mexico	TOT	March 2006	Hourly	5.4-6.4	0.6-2.1	Yu et al., 2009
Mumbai	TOT	March-May 2007, October-November 2007 and December-January 2007-2008	15 days in a season	20.4-31.3	5.0-9.2	Villalobos et al., 2015
New Delhi	TOR	January 2013 -May 2014	N=95	17.7	10.3	Sharma and Mandal, 2017
New York	TOT	March 2017-February 2018	Once every 3 days	2.88	0.63	US EPA*
Paris	TOT	from 11 September 2009 to 10 September 2010	Once everyday	3.0	1.4	Bressi et al., 2013
São Paulo	TOT	2014	Once each Tuesday	10.2	7	Pereira et al., 2017
Shanghai	TOT	from July 2013 to June 2014	Hourly	8.4	3.1	Xu et al., 2018
Soul	TOT	from January 2014 to December 2014	Hourly	4.1	1.6	Park et al., 2015
Tianjin	TOR	from Dec 23, 2013, to Jan 16, 2014	N=25	30.53	8.21	Wu et al., 2015
Tokyo	TOT	from July 27 to August 15, 2014	Once everyday	2.2	0.6	Miyakawa et al., 2016
Toronto	TOT	December 1, 2010-November 30, 2011	Hourly	3.39	0.5	Sofowote et al., 2014
Wuhan	TOT	From August 2012 to July 2013	Once every six days	16.9	2.0	Zhang et al., 2015
Xi'an	TOR	Four months of 2010	N=56	18.6	6.7	Wang et al., 2015

1058

*<https://aqs.epa.gov/api>

1059

TOR: thermal-optical reflectance; TOT: thermal-optical transmittance

1060 Table 3. OC/EC ratios in main domestic and foreign cities.

Cities		Period	Method	OC/EC	References
		1999-2000	TOR	2.7	He et al., 2001
		2000	TOT	7.0	Song et al., 2006
		2001-2002	EA	2.6	Duan et al., 2006
		2005-2006	TOT	3.0	Yang et al., 2011b
		2008	TOT	2.2	Yang et al., 2011a
		2008-2010	TOR	4.4	Hu et al., 2015
Domestic cities	Beijing	2009-2010	TOR	2.9	Zhao et al., 2013
		2009-2010	TOT	3.4	Zhang et al., 2013
		2012-2013	TOT	7.0	Wang et al., 2016c
		2013	TOT	5.0	Ji et al., 2018
		2014	TOT	4.8	Ji et al., 2018
		2013	TOT	3.6	This study
		2014	TOT	3.0	This study

	2015	TOT	3.0	This study
	2016	TOT	3.0	This study
	2017	TOT	2.9	This study
Baoji	March 2012 - March 2013	TOR	5.3	Niu et al., 2016
	2009-2010 annual	TOR	2.5	Tao et al., 2013
Chengdu	2009–2013	TOR	4.4	Shi et al., 2016
	2011 annual	TOR	2.4	Tao et al., 2014
	2012-2013 annual	TOT	4.1	Chen et al., 2014
	2005-2006 annual	TOR	4.7	Yang et al., 2011b
Chongqing	2012-2013 annual	TOT	3.8	Chen et al., 2014
	May 2012-May 2013	TOT	3.6	Chen Y. et al., 2017
Ya'an	June 2013 - June 2014	TOT	13.3	Li et al., 2018
Hangzhou	2004-2005 annual	EA	2.0	Liu G. et al., 2015
Hongkong	July - October 2014 and December 2014 - March 2015	TOR	3.5	Chen et al., 2018
Lhasa	May 2013 - March 2014	TOR	1.5	Li et al., 2016

Nanjing	2014 annual	TOT	1.8	Chen D. et al., 2017
	2011-2014 annual	TOR	2.6	Li et al., 2015
Ningbo	2009-2010 annual	TOR	2.8	Liu et al., 2013
Neijiang	2012-2013 annual	TOT	4.5	Chen et al., 2014
Qingling	March 2012 - March 2013	TOR	6.3	Niu et al., 2016
Shanghai	2009 annual	TOR	3.4	Zhao et al., 2015a
	2011	TOT	2.6	Chang et al., 2017
	2012	TOT	2.9	Chang et al., 2017
	2012 annual	TOR	5.4	Zhao et al., 2015b
	2013	TOT	3.4	Chang et al., 2017
Shijiazhuang	Four seasons (2009-2010)	TOR	2.7	Zhao et al., 2013
Tianjin	2009-2010	TOR	2.7	Zhao et al., 2013
Xi'an	2010 annual	TOR	2.7	Wang et al., 2015
	March 2012 - March 2013	TOR	4.0	Niu et al., 2016
	March 2012 - March 2013	TOR	4.0	Niu et al., 2016

		March 2012 - March 2013	TOR	3.8	Niu et al., 2016
		December 2014 - November 2015	TOT	10.4	Dai et al., 2018
	Weinan	March 2012 - March 2013	TOR	4.4	Niu et al., 2016
	Wuhan	From August 2012 - July 2013	TOT	8.5	Zhang et al., 2015
	Athens	May 2008 - April 2013	TOT	3.9	Paraskevopoulou et al. 2014
	Los Angeles	March 2017-February 2018	TOT	5.1	US EPA*
	New Delhi	January 2013 -May 2014	TOR	1.7	Sharma and Mandal, 2017
	New York	March 2017-February 2018	TOT	4.6	US EPA*
Foreign cities	Paris	September 11, 2009 - September 10, 2010	TOT	2.1	Bressi et al., 2013
	São Paulo	2014	TOT	1.5	Pereira et al., 2017
	Seoul	January 2014 - December 2014	TOT	2.6	Park et al., 2015
	Tokyo	July 27 - August 15, 2014	TOT	3.7	Miyakawa et al., 2016
	Toronto	December 1, 2010-November 30, 2011	TOT	6.8	Sofowote et al., 2014

1061 *<https://aqs.epa.gov/api>

1062 TOR: thermal-optical reflectance; TOT: thermal-optical transmittance; EA: elemental analysis